

www.acsnano.org

The Critical Roles of Water in the Processing, Structure, and Properties of Nanocellulose

Shuangshuang Jing, Lianping Wu, Amanda P. Siciliano, Chaoji Chen,* Teng Li,* and Liangbing Hu*



Downloaded via UNIV OF MARYLAND COLG PARK on August 22, 2024 at 02:32:23 (UTC). See https://pubs.acs.org/sharingguidelines for options on how to legitimately share published articles.

Cite This: ACS Nano 2023, 17, 22196-22226

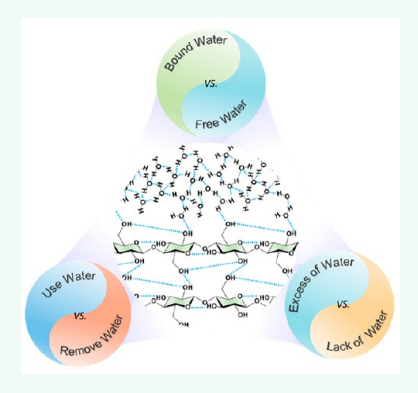


ACCESS I

III Metrics & More

Article Recommendations

ABSTRACT: The cellulose industry depends heavily on water owing to the hydrophilic nature of cellulose fibrils and its potential for sustainable and innovative production methods. The emergence of nanocellulose, with its excellent properties, and the incorporation of nanomaterials have garnered significant attention. At the nanoscale level, nanocellulose offers a higher exposure of hydroxyl groups, making it more intimate with water than micro- and macroscale cellulose fibers. Gaining a deeper understanding of the interaction between nanocellulose and water holds the potential to reduce production costs and provide valuable insights into designing functional nanocellulosebased materials. In this review, water molecules interacting with nanocellulose are classified into free water (FW) and bound water (BW), based on their interaction forces with surface hydroxyls and their mobility in different states. In addition, the waterholding capacity of cellulosic materials and various water detection methods are also discussed. The review also examines water-utilization and water-removal methods in the



fabrication, dispersion, and transport of nanocellulose, aiming to elucidate the challenges and tradeoffs in these processes while minimizing energy and time costs. Furthermore, the influence of water on nanocellulose properties, including mechanical properties, ion conductivity, and biodegradability, are discussed. Finally, we provide our perspective on the challenges and opportunities in developing nanocellulose and its interplay with water.

KEYWORDS: nanocellulose, biomass, hydrogen bonding, water absorption, dewatering, mechanical property, ion conductivity, biodegradability

ellulose, one of the most abundant biomass materials, has been thoroughly investigated due to its inexpensiveness, sustainability, excellent mechanical properties, biocompatibility, and biodegradability. 1,2 Cellulose can be produced from a variety of sources, including bacteria, algae, wood, hemp, and herbs. Wood, the most easily accessible of these materials, has been broadly pulped to generate cellulose fibrils (Figure 1A). Specifically, the process starts with cooking and bleaching wood using water, which is the foremost solution of chemicals and the medium for heat transfer for facilitating lignin removal. The following steps involving screening and washing rely on water to clean the pulp. The production of pulp incurs significant water consumption; even the thermomechanical pulp with the lowest water consumption still necessitates 4 tons of water per ton of dried pulp (Figure 1B).^{3,4} Compared with unbleached pulps, the bleached pulp requires more water to help further remove the residue lignin and purify the cellulose. Furthermore, the production of pulp from straw and bagasse requires more water than those made

Water plays a crucial role not only in pulp production but also in dispersion and transportation processes. Industries such

as papermaking and textiles heavily rely on water to beat and homogenize cellulose pulp, where water acts as an energy and mass transfer agent, ensuring the formation of uniform and stable cellulose fiber suspensions. However, a large amount of water in cellulose suspensions must be removed while producing dry cellulose products, leading to an additional energy consumption. In these water-removal procedures, water is potent. The surface tension of water in cellulose suspensions helps remold interactions between cellulose, thus facilitating the building of various cellulosic materials with different microscopic and macroscopic structures.⁵

Furthermore, the properties of cellulosic materials are closely related to their water content. As depicted in Figure 1C, cellulose fibers within plant cell walls exhibit a hierarchical arrangement that includes cellulose fibrils ranging from the

Received: July 22, 2023 Revised: October 22, 2023 Accepted: November 1, 2023 Published: November 7, 2023





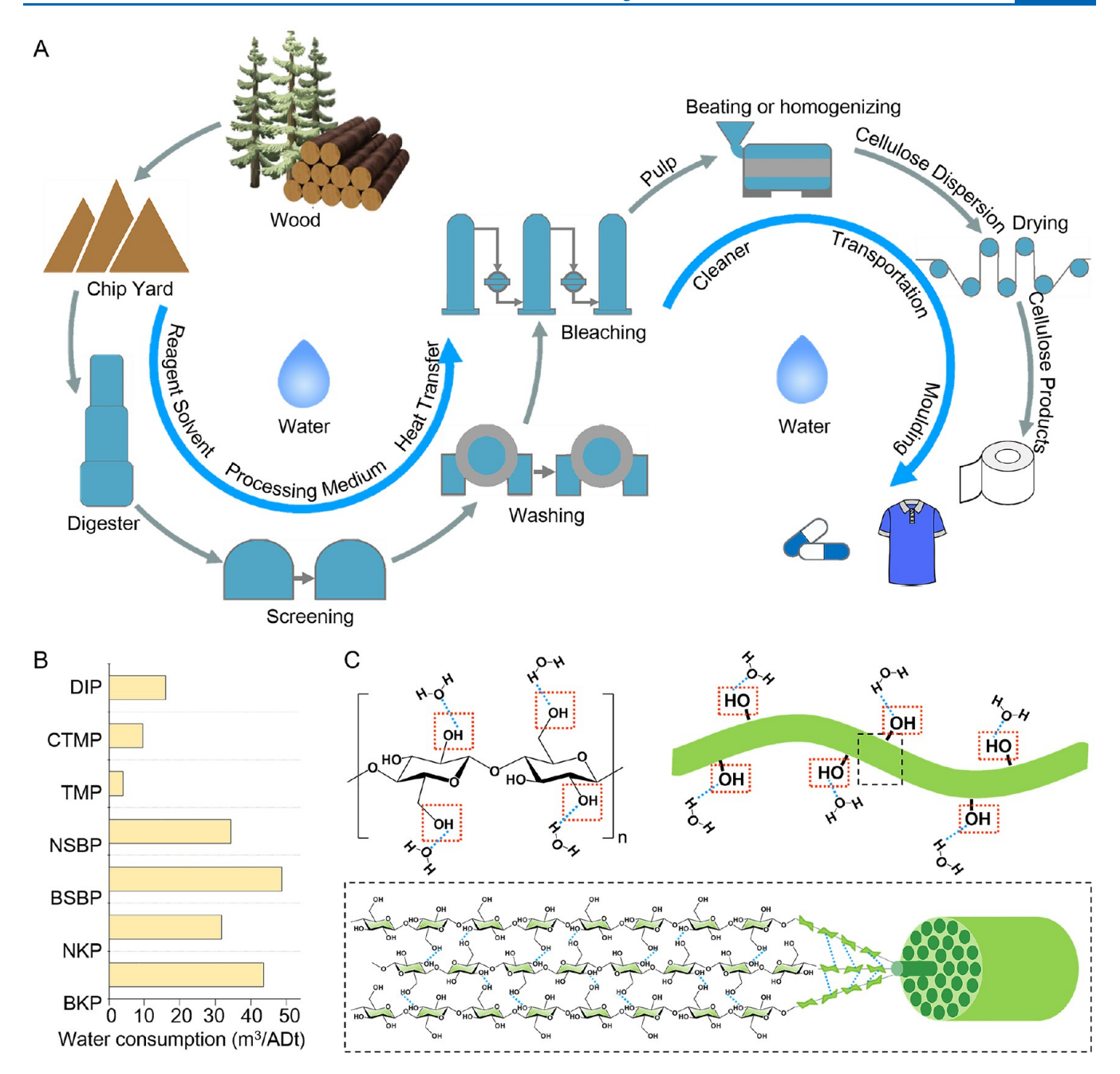


Figure 1. The relationship between water and cellulose in the cellulose industry is inseparable due to the hydrophilic nature originating from the chemical structure of cellulose. (A) The cellulose manufacturing, processing, transport, and molding process relies heavily on water. Reproduced with permission under Creative Commons Attribution (CC BY) license (https://creativecommons.org/licenses/by/4.0/) from ref 12. Copyright 2020 MDPI. (B) The overall water consumption amount in the production of waste paper deinked pulp (DP), chemithermomechanical pulp (CTMP), thermomechanical pulp (TMP), natural sulfate bamboo pulp (NSBP), bleached sulfate bamboo pulp (BSBP), natural Kraft pulp (NKP), and bleached Kraft pulp (BKP). Reproduced with permission for ref 3. Copyright 2018 Elsevier. Reproduced with permission under Creative Commons Attribution 4.0 International (CC BY 4.0) license (https://creativecommons.org/licenses/by/4.0/) from ref 4. Copyright 2015 Publications Office of the European Union. (C) The chemical constructions of cellulose chains and schematic description of cellulose fibrils.

nanoscale to microscale. These microfibrils can be further divided into elementary fibrils, each with a diameter of 1.5-3.5 nm, and exhibit both crystalline and amorphous regions. At a finer scale, a single cellulose chain consists of numerous β -glucopyranose rings linked to each other via 1,4-glycosidic bonds. Abundant hydroxyl groups on β -glucopyranose rings are dominant functional groups that provide hydrogen bonds linking to other substances with polar functional groups,

typically referring to water molecules and other cellulose chains in this system. As a result, water molecules tend to be absorbed onto the surfaces of polar hydroxyl groups and hydrate the surfaces of the materials. In addition, water molecules can penetrate the gap and pores between cellulose fibrils to alter the structure and other properties, such as mechanical properties, ion conductivity, and degradability.

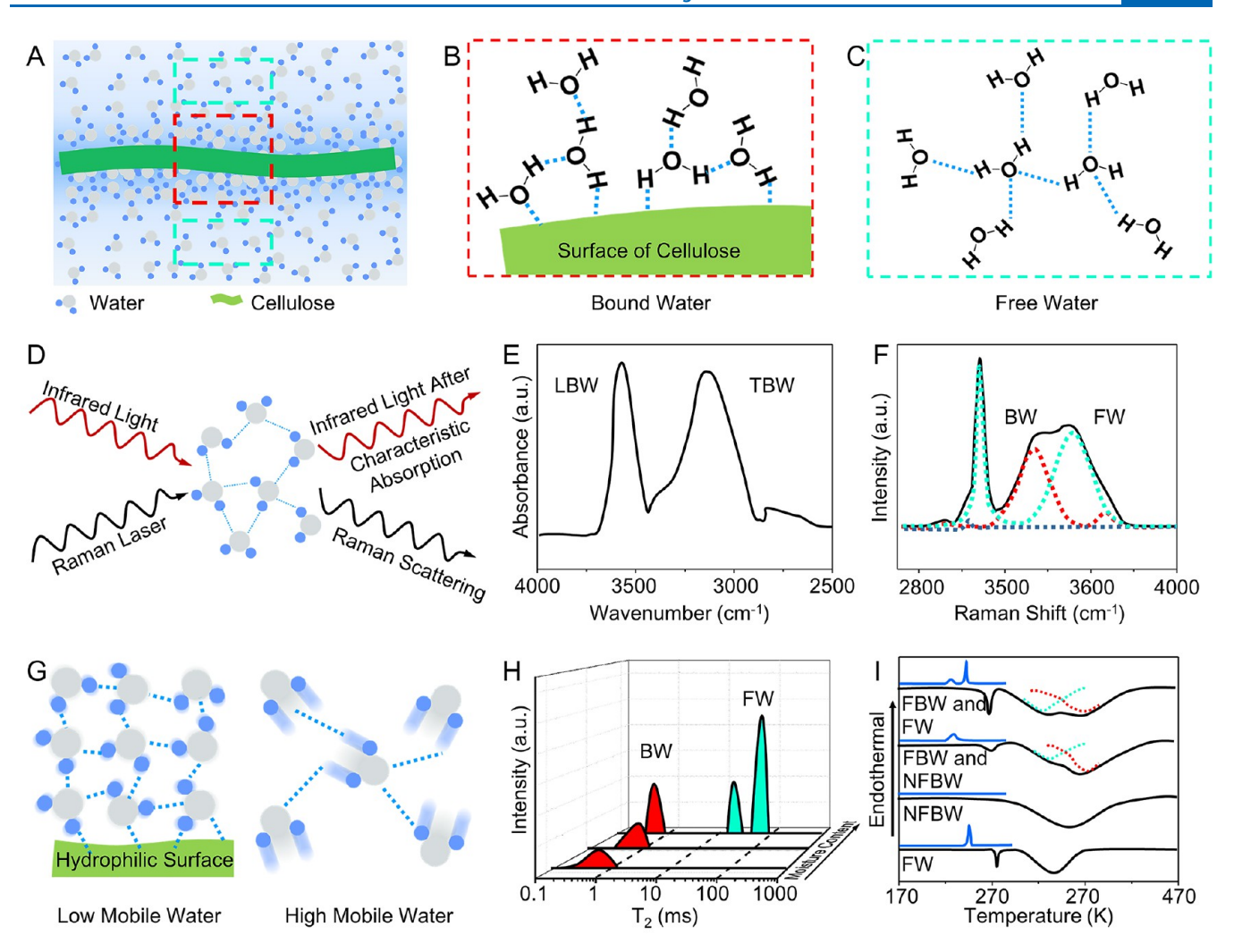


Figure 2. Definition, properties, and detection of bound water and free water. (A) The diagram shows water aggregation around the cellulose fiber. (B, C) Water molecules firmly bound on the surface of the fiber are BW (B), and those that are distant enough from the cellulose and isolated from hydroxyl are FW (C). (D) Schematic description of the vibration of O-H under infrared light irradiation and a Raman laser. (E, F) The vibration of the O-H bond of water can be detected, and the results are shown for (E) infrared and (F) Raman spectra. (E) is reprinted with permission from ref 16. Copyright 2004 Elsevier. (F) is reprinted with permission from ref 21. Copyright 2009 AIP Publishing. (G) Schematic description of the different mobilities of water in cellulosic materials. (H, I) BW and FW can be distinguished by ¹H NMR (H), DSC, and DTA (I) according to the different mobilities. (H) is reprinted with permission from ref 24. Copyright 2019 Elsevier. (I) is reprinted with permission from ref 26. Copyright 1988 Elsevier.

In recent years, studies of cellulosic materials have been mainly focused on nanoscale materials, including cellulose nanofibers (CNFs) and cellulose nanocrystals (CNCs) (in this article, we use the general term "nanocellulose" to describe them) with exceptional properties of both cellulose and nanomaterials. In particular, nanocellulose has shown great potential in various applications such as bioplastics, medication and cosmetics, optical devices, energy storage, environmental remediations, water purification, and so on. However, the intrinsic hydrophilic feature of nanocellulose and the substantial water consumption during its manufacturing and processing bring critical challenges concerning transportation, drying, storage, and lifetime. Addressing these challenges is crucial to fully exploit the potential of nanocellulose composites and advance their industrial applications. 11 Hence, to reduce production costs and inspire the design of nanocellulose-based functional materials, it is crucial to have an in-depth understanding of the interplay between nanocellulose and water.

This review provides a comprehensive overview of the fundamental understanding of free and bound water in nanocellulose materials and the necessary analysis methods to detect and differentiate them. Then, we describe the design and processing principles of nanocellulose materials by adding or removing water, emphasizing the interplay between nanocellulose and water during material processing. Meanwhile, we summarize the significant influence of water (excess water vs lacking water) on the properties and performance of cellulose-based functional materials. Finally, future perspectives on potential challenges and opportunities related to the nanocellulose—water interplay are provided.

FREE WATER AND BOUND WATER

Due to its polarization, water absorbed on the surface of hydrophilic materials is generally made of multiple layers. Cellulose, as a typical hydrophilic material, has also demonstrated a multilayered absorbed water structure. Typically, the first hydration layer is bound to hydroxyl groups

Table 1. Detection Methods Applied in the Identification of Free and Bound Water, Hydrogen Bonding Analysis, Moisture Analysis, and Visualization of Water Hydrogen Bonding

materials	methods	water and hydrogen bonding analysis	ref
paper	FTIR	TBW (3200 cm ⁻¹)	16
	moisture control	LBW (3600 cm ⁻¹)	
	deconvolution		
bPEI/TOUS-CNFs	FTIR-ATR	O-D stretching (2000-2800 cm ⁻¹)	17
	deuterium labeling	D-O-D bending, 1210 cm ⁻¹	
methylcellulose	FTIR	BW (1640.3 cm ⁻¹)	18
	moisture control algorithm fitting	FW(1655.8 cm ⁻¹) O-H bending red shift with increasing moisture content	
microcrystalline cellulose	ATR/IR	O-H stretching intensity decreased with bulk water evaporation	19
	drying control	5	
	PCA, 2DCOS		
	NID	the intensity in the section of 7200 (200 cm ⁻¹) in section with the increase in	20
microcrystalline cellulose	NIR	the intensity in the region of 7200–6200 cm ⁻¹ increases with the increase in moisture content	20
	moisture control		
	PCA, 2DCOS		
poly <i>n,n</i> -dimethylacrylamide	Raman	TBW (3050, 3233, 3401 cm ⁻¹)	21
hydrogel		I DIV (2514-2620 -1)	
	gaussian function fitting	LBW (3514, 3630 cm ⁻¹)	
poly(vinyl alcohol) hydrogel	Raman	LBW (3612 cm ⁻¹)	22
	Gaussian function fitting	TBW (3240, 3411 cm ⁻¹)	
bacterial cellulose	nautron scattering	NFBW (250 K)	23
Dacterial Centiose	neutron scattering deuterium labeling	FBW (265 K)	23
	temperature control	(
	•		
corn straw cellulose powder	LF-NMR	BW $(T_2 < 10 \text{ ms})$	24
	moisture control	TBW $(T_2 \approx 0.7 \text{ ms})$	
		LBW $(T_2 \approx 1.5 \text{ ms})$	
		FW $(T_2 \approx 40 \text{ ms})$ bulk water $(T_2 \approx 1000 \text{ ms})$	
		bulk water $(1_2 \sim 1000 \text{ ms})$	
filter paper	TD-NMR	TBW $(T_2 = 1 \text{ ms})$	25
	moisture control	LBW $(T_2 = 3 \text{ ms})$	
1/1 1 , \ 11.1	DEA DOC TOA	$FW (T_2 = 110 \text{ ms})$	26
poly(hydroxystyrene) cellulose diacetate c	DTA, DSC, TGA, moisture control	DSC (crystallization)	26
		NFBW (first-order transition of water was not observed)	
		FBW (a small broad peak at about 235 K)	
		FW (sharp peak at about 255 K)	
		DTA (vaporization)	
		pure water (sharp peak around 270 K and broad peak around 330 K) NFBW (broad peak at around 360 K)	
		NFBW and FBW (small peak at around 270 K, broad peak around 330 K with	
		shoulder at 330 K)	
		NFBW, FBW, and FW (sharp peak around 270 K, broad peak around 330 K with shoulder at 330 K)	
		TGA (vaporization)	
		BW (second step of the weight loss)	
Paper	TGA-DSC, FTIR, moisture control	content of FW, LBW, TBW	27
1	,	FW (3610 cm ⁻¹)	
		LBW (3510 cm ⁻¹)	
		medium strength hydrogen bounds (3360 cm ⁻¹)	
		TBW (3070 cm ⁻¹)	
paper	HRI-TGA, temperature control	hard-to-remove water	28
	, ,		

Table 1. continued

materials	methods	water and hydrogen bonding analysis	ref
wood/CNF	HRI-TGA	hard-to-remove-water	29
wood	NIR-HIS drying control	spatial resolution: 125 μ m visualization of moisture distribution dynamic change of FW and BW	30
apple and potato cells	CRM	spatial resolution: 1 μ m visualization of hydrogen bonding states of water and moisture distribution	31, 32
wood	CRM deuterium labeling moisture control	spatial resolution: $<0.3 \mu m$ moisture distribution	33
soft wood	neutron radiography	spatial resolution: $80-100~\mu\mathrm{m}$ spatial distribution of moisture	34
nanocellulose treated cotton	neutron radiography	spatial resolution: 53 μ m diffusion of moisture	35
cellulose foam	X-ray computed tomography frozen	spatial resolution: 90 μ m density profiles of ice	36
sea cucumber	NMR and MRI rehydration	distribution of FW and BW FW: T_2 weighted images BW: T_1 weighted images	37
paper	MRI moisture control	spatial resolution: 10 um diffusion of moisture	38
cellulose slurry	NMR, MRI drying control	spatial resolution: 1 mm distribution of moisture, FW and BW	39
CMC/surimi gels	NMR, MRI	distribution of BW and FW T_2 relaxation time profiles, water distribution	40
oil-paper	terahertz time-domain spectroscopic imaging	distribution of moisture	41

on cellulose and introduces the absorption of the second layer, which also increases the absorption of the third and more layers of water. A previous simulation study reveals that the first hydration layer extends up to 0.36 nm from cellulose, while the second layer can reach up to 0.65 nm, and the third layer can extend over 0.8 nm from cellulose. 13 Although water hydration is subdiffusive, the polarized water layer could be extended from the nanoscale to the microscale. 14 As illustrated in Figure 2A, when a cellulose fibril is isolated and stably dispersed in water, according to the electrical double-layer model, the hydroxyl groups in cellulose would undergo slight ionization in water, creating a negatively charged surface that attracts counterions and inducing a diffusion layer composed of hydronium and hydroxide ions, which are loosely associated on the surface of cellulose. 15 Water molecules absorbed on cellulose through hydrogen bonding and polarization with less mobility are named bound water (BW) (Figure 2B), while water molecules that are sufficiently distant from polar groups on cellulose with mobility and thermal properties close to those of bulk water are categorized as free water (FW) (Figure 2C). It is worth noting that the mobility of BW at varying layers differs due to interactions between water and cellulose.

According to the interaction strength between water and cellulose, BW could be recognized as tightly bound water (TBW) or loosely bound water (LBW). Differentiating between BW and FW in cellulosic materials will be beneficial for understanding the corresponding physical and chemical properties of nanocellulose materials.

Detection Methods. To identify BW and FW, various analysis methods have been developed, including infrared (IR) spectroscopy, Raman spectroscopy, neutron scattering, nuclear magnetic resonance (NMR), differential scanning calorimetry (DSC), differential thermal analysis (DTA), and thermal gravimetric analysis (TGA). Based on the detection mechanism, these methods can be categorized into two groups: spectroscopy methods that investigate the O–H vibrations and other techniques that monitor water mobility. Table 1 summarizes the detection methods employed for the identification of FW and BW, the analysis of water hydrogen bonding, moisture analysis, and the visualization of water hydrogen bonding.

Interactions between water molecules and water-cellulose are predominantly governed by the hydrogen bonding of O-H groups. Spectroscopy methods, including IR, Raman, and

neutron scattering, have been used to investigate the O-H vibration under the irradiation of certain types of light (Figure 2D). In particular, IR spectroscopy has been widely used to study water dynamics and structure in hydrophilic polymers. However, it is hard to distinguish the intermolecular hydrogen bonding of cellulose and the hydrogen bonding between cellulose and water due to the overlapping peaks of O-H stretching. For example, Olsson et al. 16 recorded the Fourier transform infrared (FTIR) spectra of water and paper under different relative humidities (RHs). A computer deconvolution analysis was introduced to give more precise information regarding water assignment in the O-H region. As shown in Figure 2E, peaks at 3200 and 3600 cm⁻¹ in the spectra development are associated with TBW and LBW, respectively. Besides, Watanabe et al. 19,20 combined a principal component analysis (PCA), generalized two-dimensional correlation analysis (2DCOS), and second-derivative analysis to analyze the attenuated total reflection infrared (ATR/IR) spectroscopy of wet microcrystalline cellulose (MCC) and study the water dynamics during the drying process. A slight drop in the broad band at 3390 cm⁻¹ was identified during the first drying stage, indicating the evaporation of bulk FW.

Raman spectroscopy, similar to IR spectroscopy, is a valuable tool for investigating water by analyzing the scattering of O–H bond scattering. It offers the advantage of studying samples in aqueous environments, making it well-suited for examining the water distribution in hydrogels. Ikeda-Fukazawa et al. 21,22 incorporated computer deconvolution with Gaussian function matching to analyze the O–H stretching mode of water through Raman spectroscopy. The broad band at around 3400 cm⁻¹ is associated with the vibration of the water molecules (Figure 2F). The O–H stretching mode is further analyzed by Gaussian function fitting, and peaks at 3240 and 3411 cm⁻¹ are assigned to in-phase and out-of-phase modes of the O–H stretching vibration of water molecules with four hydrogen bonds.

On the other hand, the peak at 3612 cm⁻¹ represents the weakly or non-hydrogen-bonded water's O-H stretching, where water's hydrogen bonds are partly or entirely disrupted. Neutron scattering is sensitive to hydrogen atoms and is used to study the cellulose structure with a molecular dynamics (MD) simulation. Quasi-elastic neutron scattering (QENS) shows the relaxation and diffusive dynamics of water in cellulosic materials and distinguishes rotational motions of hydrated polysaccharides from long-range translational dif-fusion of water. 42 O'Neill et al. 23 recognized the nonfreezable water absorbed on cellulose and the confined water accumulating in narrow spaces between fibrils with the combination of deuterium labeling, QENS, and MD. The analysis of QENS shows that the water diffusion coefficient of nonfreezable water doubles with a temperature increase from 250 to 265 K, while water molecules confined in cell lumens remain frozen.

NMR, DSC, DTA, and TGA methods are often used to investigate the structure, distribution, and quantity of water molecules. As illustrated in Figure 2G, water molecules bound to the cellulose surface are limited by hydrogen bonds, and thus, they require more energy to be activated, causing lower mobility. In comparison, water molecules that interact with each other and are negligibly affected by the cellulose surface show a higher mobility. NMR is commonly used to study water in wood materials, 43,44 muscular tissue, 45 and hydrophilic biocompatible polymers. 46 Different bonding strengths

between cellulose and water will induce different spin—spin relaxation times (T_2) in the $^1\mathrm{H}$ NMR spectra through low-field NMR (LF-NMR) or time domain NMR (TD-NMR). With tighter hydrogen bonding between water and cellulose, the spectra show shorter T_2 values. Also, the mobility of BW leaves a gentle peak shorter than 10 ms in the NMR relaxation time ranges. In comparison, the mobility of FW exhibits sharp and multiple peaks with T_2 values longer than 10 ms, as shown in Figure 2H. In summary, T_2 relaxation analysis detects and analyzes water in cellulosic materials according to its mobility and therefore helps to locate and study the change of water state during hydrolysis, drying, or wetting process.

DSC can distinguish water by recording the exothermic and endothermic peaks during the cooling and melting process. In contrast, TGA and DTA can record weight and phase changes during evaporation. 26,27,48,49 In the cooling process, the exothermic case of water was detected and recorded by DSC with temperature cooling from 280 to 170 K.²⁶ FW freezes at a temperature similar to that of bulk water. Meanwhile, the BW shows a supercooling phenomenon induced by the interaction between water and cellulose, resulting in its freezing at a lower temperature. To illustrate this, Figure 2I summarizes the typical DSC spectra and peaks of water in hydrophilic materials. Accordingly, water that is bound tightly to cellulose and does not show the first-order thermodynamic phase transition will not be detected by DSC and is named nonfreezable bound water (NFBW). Water that freezes at a temperature lower than the FW is recognized as freezable bound water (FBW).

The melting process of water is more complicated than the cooling and evaporation processes. Due to the non-first-order thermodynamic phase transition behavior, NFBW also shows no DSC curves during the melting process. With a water content lower than 50%, the FBW shows a melting temperature lower than that of bulk water. In contrast, FW shows a melting temperature close to that of bulk water (around 0 $^{\circ}$ C).^{48–50} When the water content becomes higher (materials like hydrogel), the melting peaks of FBW and FW in swollen materials gradually merge into a broad band at a higher melting range. 48-50 Similar to the cooling and melting processes, FW evaporates like bulk water. Instead, BW shows a superheating phenomenon and evaporates at temperatures of >100 °C with more endothermic energy. The DTA result shown in Figure 2I indicates that an endothermic peak associated with FBW will appear at a temperature lower than the peak of NFBW and shift toward the peak of FW as the water content rises.

TGA is also expected to recognize and measure the water content in hydrophilic materials. However, water starts evaporating as soon as the ice melts, which results in water contents calculated from TGA measurements that are less reliable than those of DSC and DTA. Although water loss at a temperature higher than 100 °C, recognized as BW, is more reliable, it is more likely to be measured in materials with strong hydrophilic groups, such as hydroxyl groups, on cellulose. Therefore, the TGA of water is widely used in the paper industry. Water determined by high-resolution isothermal TGA (HRI-TGA) in the paper industry is called hard-to-remove water, which is also a kind of BW achieved by analyzing the first- and second-derivative curves. In brief, the amount of BW calculated through DTA, DSC, and TGA agrees fairly well when testing the strong hydrophilic groups,

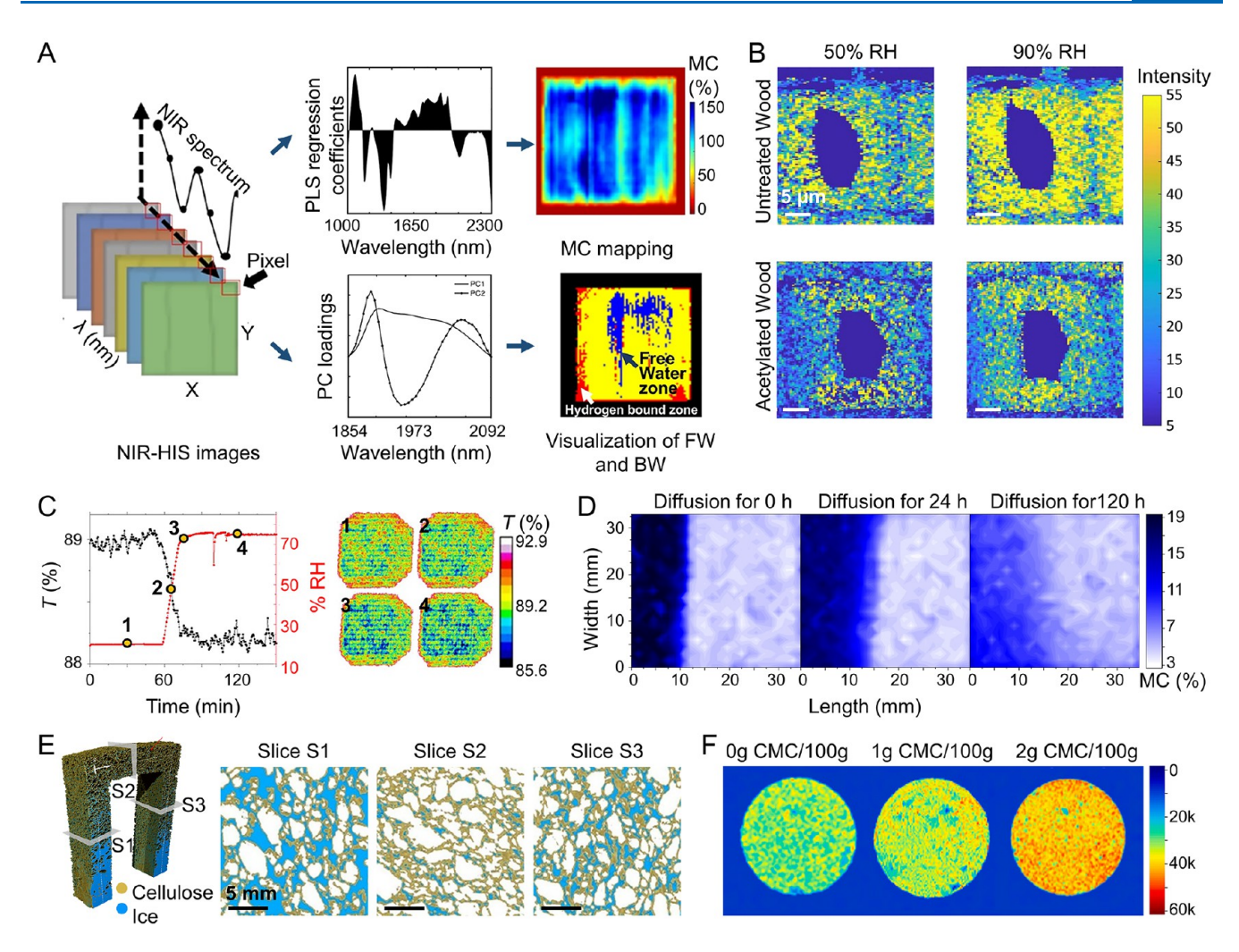


Figure 3. Visualization of hydrogen bond, moisture content, and distribution in cellulosic materials. (A) Investigating hydrogen bonding and differentiating FW and BW by NIR-HIS assisted with PLS and PCA. Reprinted with permission from ref 30. Copyright 2021 Springer Nature. (B) Combination of CRM and a moisturizing system with deuterium oxide to in situ map water distribution in wood under different RH conditions. Reprinted with permission under Creative Commons Attribution license (CC BY) (https://creativecommons.org/licenses/by/4.0/) from ref 33. Copyright 2022 Frontiers. (C) Tracking moisture diffusion in untreated and nanocellulose-consolidated cotton canvases by neutron radiography. Reprinted with permission under Creative Commons Attribution 4.0 International license (https://creativecommons.org/licenses/by/4.0/) from ref 35. Copyright 2021 American Chemical Society. (D) Visualization of moisture diffusion in oil paper insulation by THz. Reprinted with permission from ref 41. Copyright 2023 IEEE. (E) Investigating the capillary flow through the micro pores in the cellulose foams via X-ray computed tomography. Reprinted with permission under Creative Commons CC-BY license (https://creativecommons.org/licenses/by/4.0/) from ref 36. Copyright 2022 Elsevier. (F) Visualization of moisture content in gels added with CMC by MRI. Reprinted with permission from ref 40. Copyright 2023 Elsevier.

such as hydroxyl groups. However, the results may vary when testing weak hydrophilic groups such as acetoxyl.²⁶

Visualization of Water Hydrogen Bond. Based on the practical and nondestructive detection of hydrogen bonding and identification of FW and BW in cellulosic materials, infrared techniques can also be used to visualize FW and BW distribution. Ma et al.³⁰ visualized the dynamic change in FW and BW within wood using NIR hyperspectral imaging (NIR-HSI). They employed partial least-squares (PLS) regression analysis and principal component analysis (PCA) to generate the maps of moisture content (MC), FW, and BW distribution. Similarly, based on NMR and Raman, magnetic resonance imaging (MRI) and confocal Raman microspectroscopy (CRM) have been utilized to visualize moisture in materials, especially cellular food materials. 31,32,37,51 T_1 (spin-lattice relaxation time) and T_2 -weighted MRI images, 37 as well as the

CRM image processed using an iterative computational algorithm, 31 can effectively visualize the distribution of FW and BW in cellular food. However, their application in cellulosic material analysis requires further verification study. Setting aside the purpose of discriminating between FW and BW, as shown in Figure 3, MRI, X-ray topography, neutron radiography, and terahertz (THz) time-domain spectroscopy have found extensive use in visualizing water distribution and moisture content within cellulosic materials. 33,35,36,40 These advanced techniques can visualize samples at a resolution of 1 μ m and water at a resolution of tens of micrometers. $^{31,34-36,38,39,52-54}$

NIR-HIS and CRM are capable of assessing water content and distinguishing between FW and BW in cellulosic materials, but achieving a higher accuracy requires extensive data collection and computational processing. THz and neutron

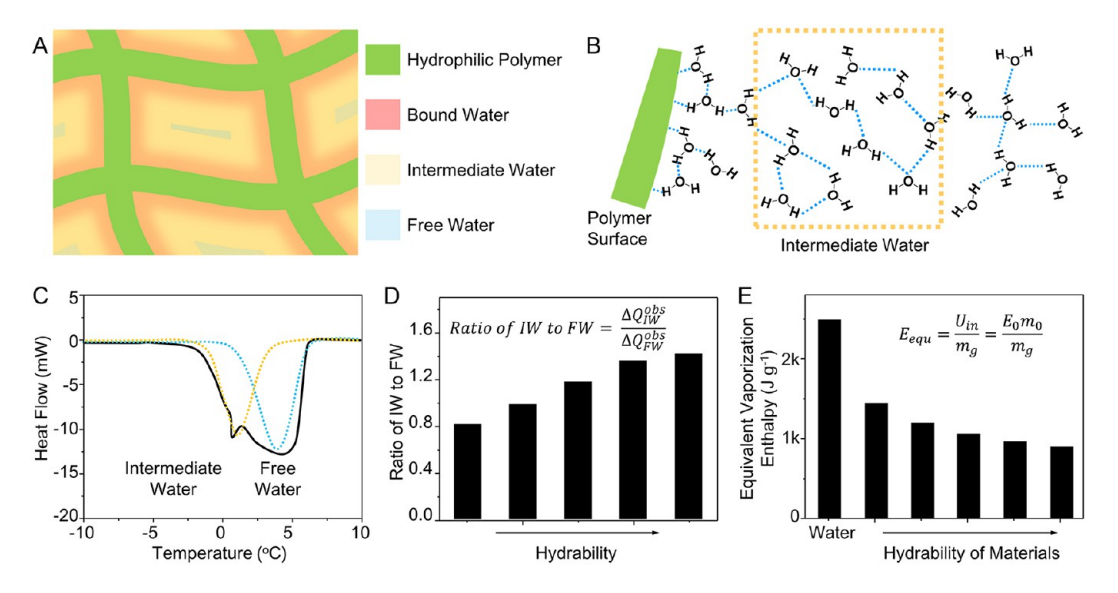


Figure 4. Intermediate water—definition, detection, and its application in solar evaporation. (A) Schematic description of water types in cellulose hydrogel. (B) Schematic illustration of the intermediate water. (C) Intermediate water and free water are recognized from DCS methods. (D) The ratio of IW to FW increases with the growing hydrability of the materials. (E) The vaporization enthalpy of water decreases with the growing ratio of the IW to FW. (C–E) from ref 50. Copyright The Authors, some rights reserved; exclusive licensee AAAS. Distributed under a CC BYNC 4.0 license (http://creativecommons.org/licenses/by-nc/4.0/). Reprinted with permission from AAAS.

radiography exhibit exceptional sensitivity to hydrogen bonding, making them advantageous for moisture detection. Furthermore, neutron radiography offers superior resolution for determining the moisture content compared to MRI and X-ray radiography. However, it is costly and needs access to large-scale research facilities equipped with neutron sources. As an emerging method, THz still demands further research and development to enhance its capabilities in detecting hydrogen bonding and moisture content within cellulosic materials.

Intermediate Water. Due to the stereo structure and chemical and physical absorption phenomenon, the actual status of water in cellulosic material is more complicated than a simple model of a single cellulose fibril in water (Figure 2A). Cellulosic materials with 3D porous and stable structures could hold water weighing more than 10-100 times their weight and maintain their figures without collapsing through chemically hydrophilic and physical capillary absorption of water. Therefore, a third part of the water molecule that interacts weakly with the polymer network and bulk water was proposed, named intermediate water (IW), as shown in Figure 4A. In contrast to FW molecules, which form four hydrogen bonds with neighboring water molecules, the IW molecules are characterized by being less attractive to each other, resulting in fewer hydrogen bonds (as depicted in Figure 4B). This properly renders IW an ideal material for solar-power water evaporation material, giving its lower evaporation enthalpy compared to bulk water.55 The IW interacts weakly with the polymer network and bulk water. It can also be recognized as LBW through Raman microscopy⁵⁰ and FBW through DSC.50,56

For instance, Zhou et al. 50 manufactured a hydrogel with controllable hydrability and discussed the relationship between IW proportion and vaporization enthalpy of hydrogels. The prominent endothermic peaks in the DSC curve are attributed to IW and FW, as shown in Figure 4C. In addition, the ratio of IW to FW is calculated as the ratio of the experimental values of IW ($\Delta Q_{\rm IW}^{\rm obs}$) and FW ($\Delta Q_{\rm FW}^{\rm obs}$) read from the fitted curves,

and this ratio increases with growing hydrability (Figure 4D). Furthermore, after recording the weight loss of materials ($m_{\rm g}$) and bulk water ($m_{\rm 0}$) in a dark space with identical power input ($U_{\rm in}$) by controlling temperature and relative humidity, the equivalent vaporization enthalpy of water in the hydrogel ($E_{\rm equ}$) that is calculated refers to the vaporization enthalpy of bulk water ($E_{\rm equ}$) according to the following formula:

$$U_{\rm in} = E_0 m_0 = E_{\rm equ} m_{\rm g}$$

To summarize, a higher ratio of IW to FW correlates with a lower equivalent vaporization enthalpy of water in hydrogels (Figure 4E). This finding is supported by research from Guan et al., ⁵⁶ who developed an advanced solar steamer using bacterial cellulose, resulting in a reduction in vaporization enthalpy. In particular, water in the CNTs/BC hydrogel is investigated through the DSC melting process, revealing IW and FW contents of 69% and 24%, respectively. The evaporation rate tested in a dark chamber shows a 60% lower equivalent vaporization enthalpy of water in the CNTs/BC hydrogel than that of bulk water. These results further support the effectiveness of the strategy to build a solar steam generator using a cellulose-based hydrogel.

Water Holding in Cellulosic Materials. Since water is ubiquitous in the environment, achieving completely dried cellulosic materials can be challenging and requires precise moisture control. Specifically, cellulose tends to absorb at least a monolayer of water molecules, even under relatively dry conditions. The number of layers increases with increasing humidity in the environment and reaches its fiber saturation point at a 100% relative humidity. This naturally absorbed water from the air is mainly considered BW, as it will not swell or destroy the appearance too much. In particular, water vapor absorption of cellulosic materials was studied by dynamic vapor absorption saturated by the weight change of materials stored in closed containers where the humidity level was controlled by a saturated salt solution. The moisture content of cellulosic materials exhibits characteristic sigmoidal

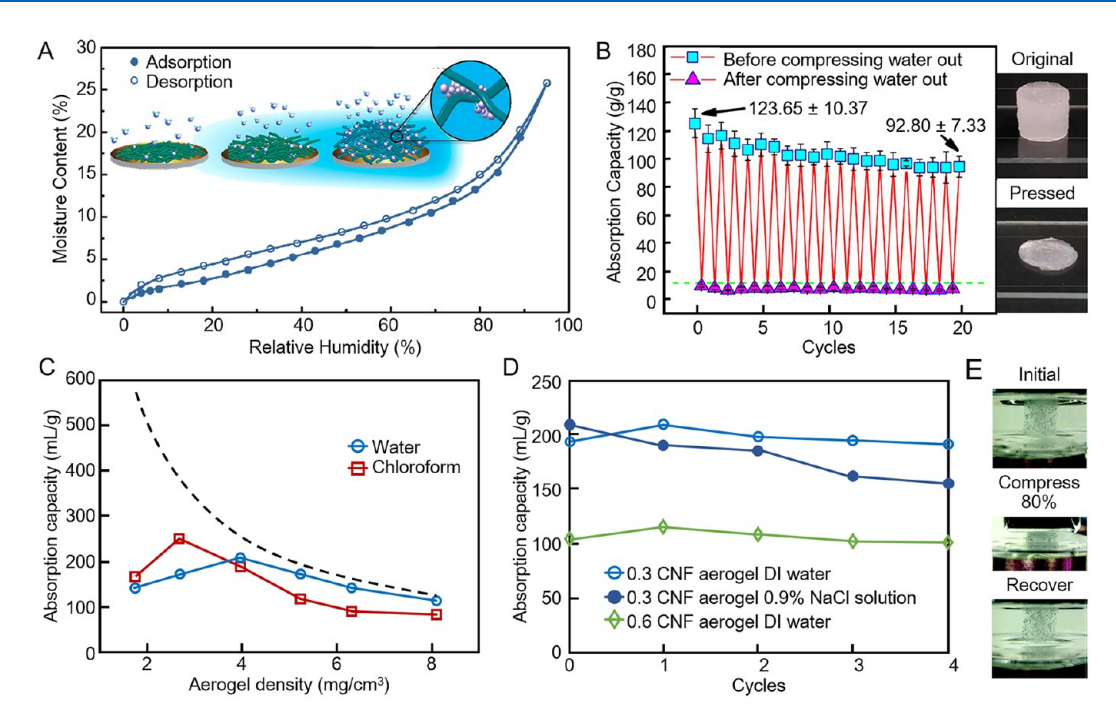


Figure 5. The water absorption properties of cellulosic materials. (A) The water uptake curve of cellulosic materials from the air in different relative humidity. Reprinted with permission from ref 62. Copyright 2017 American Chemical Society. (B) Cyclic water absorption of nanocellulose foams from liquid water and the images of samples before and after dewatering. Reprinted with permission from ref 66. Copyright 2018 American Chemical Society. (C) Water and chloroform absorption capacity as a function of CNF density. The dashed line represents calculated values. (D) Cyclic water and 0.9% NaCl absorption of 0.3 CNF (4.0 mg cm⁻³) and 0.6 CNF aerogels (8.1 mg cm⁻³). (E) Photographs of CNF aerogel compression tested under water, showing the initial status, compression at 80%, and full recovery. (C–E) are reprinted with permission from ref 67. Copyright 2013 Royal Society of Chemistry.

isotherms in the absorption and desorption processes in response to relative humidity. These moisture-humidity curves of cellulosic materials show hysteresis, indicating that water absorption and desorption processes in cellulose mainly rely on capillary condensation and evaporation. 60,61 Hakalahti et al.⁶² investigated the water vapor absorption behavior of TEMPO nanocellulose and evaluated it through the quantitative Langmuir/Flory-Huggins/clustering model and Brunauer-Emmett-Teller model. Figure 5A provides a representative water absorption model of 2D cellulosic materials made by TEMPO nanocellulose film. They found that the swelling of the film was induced by the penetration of water between the nanocellulose rather than the swelling of the nanocellulose itself. The swelling model shows that water molecules absorbed on nanocellulose go through the following three regions: the specific absorption in dry air (RH < 10%), the multilayer buildup in humid air (10% < RH < 75%), and the clustering of water molecules at high humidity levels (RH > 75%). In addition, moisture absorption predominantly occurs in the disordered regions and the surface of the crystalline regions of cellulosic materials. For example, Guo et al.⁵⁸ studied the water absorption of CNC and CNF with cellulose I and II structures and found that their equilibrium moisture contents increase with the decrease of crystallinity. They also found that the cellulose II structure absorbed more water than did the cellulose I structure during the absorption process. Additionally, the swelling of cellulose is more likely to happen in the cellulose II structure than in the cellulose I structure, resulting in a longer running time and a higher moisture content. The ratio of amorphous to crystalline

regions affects the moisture resistance of cellulosic materials, which attracts researchers to study and control the crystallinity.

However, the assembly mode of the cellulose macromolecule, which affects the specific area and content of exposed hydroxyl groups, significantly impacts the moisture absorption of cellulosic materials. First, the size of fibrils and the distribution of amorphous regions mainly manage the exposure of hydroxyl groups and distribution of BW and FW. Hatakeyama et al.⁶³ measured water distribution in CNF and MFC by DSC and reported a higher BW content in nanocellulose than in microcellulose. In another example, Mihranyan et al.⁵⁹ studied the moisture absorption of cellulosic powder with varying crystallinity. They found that microcrystalline cellulose made from a weblike Cladophora green algae with the largest pore volume and surface area showed the highest moisture absorption capacity, even when it had a high level of crystallinity, surpassing other crystalline cellulose powders with lower specific areas. Second, cellulose can retain more water with the designed scaffold and 3D structure after sufficient swelling in water. In this case, the water holding capacity (WHC), which contains both BW and FW in the materials, was raised and measured by a sieve shake method. 64,65 WHC of nanocellulose materials can be studied by subjecting them to compression and monitoring the subsequent weight change as well. However, this method requires the material to exhibit a satisfactory compressibility. Li et al.66 fabricated a nanocellulose aerogel with long-lasting water durability and enhanced hydrophilic properties through the ester cross-link. As shown in Figure 5B, the nanocellulose aerogel can hold water weighing 120 times more than the dry weight of itself and can release water quickly by compression.

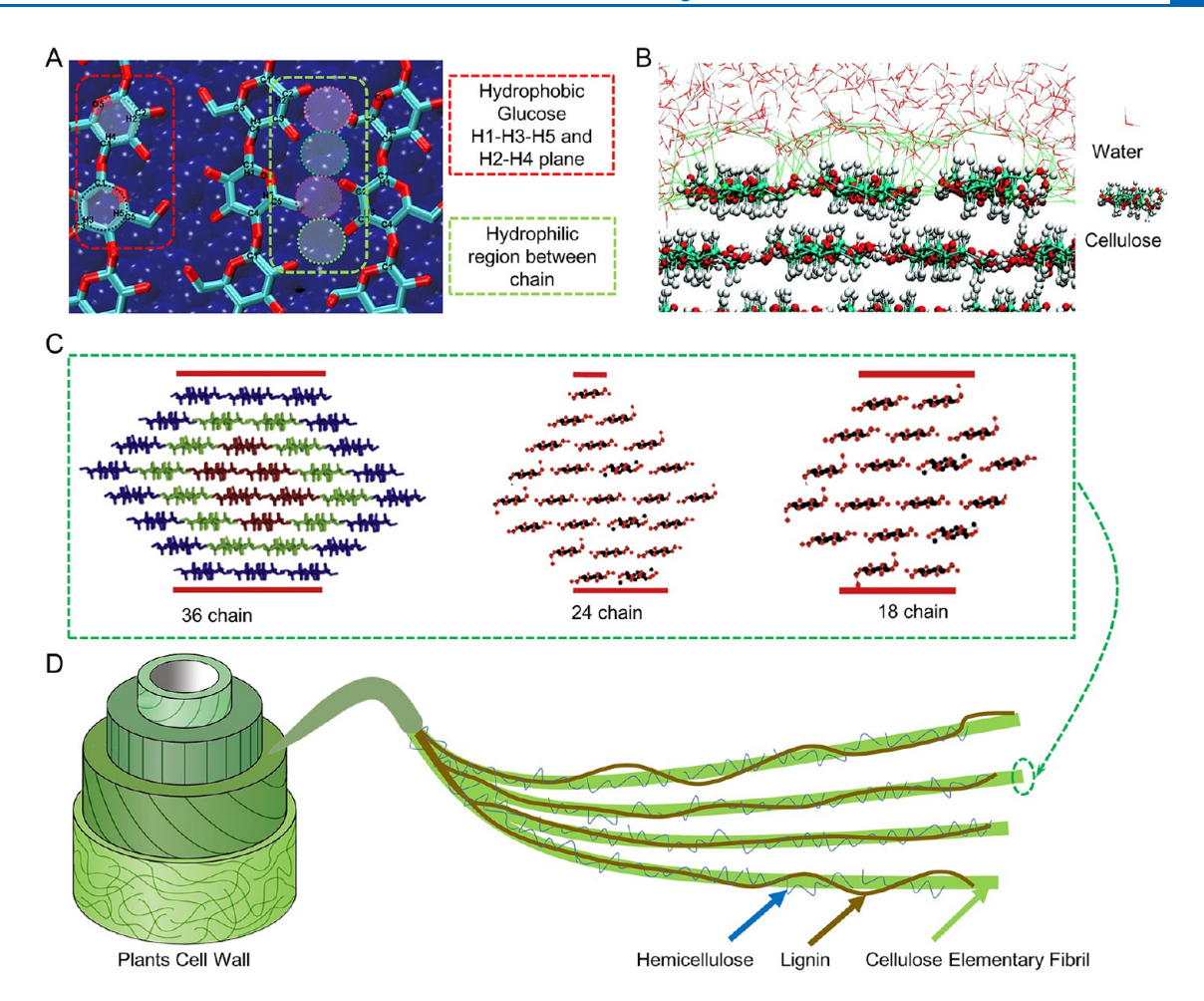


Figure 6. The hydrophobic performance of the cellulose chain and its influence on the structure of the elementary fibril and the plant cell wall. (A) Molecular structure of cellulose chain showing its hydrophobic plane and a hydrophilic region. Reprinted with permission from ref 75. Copyright 2014 American Chemical Society. (B) A snapshot of the molecular dynamics simulation of water near the hydrophobic surface of cellulose Iα. Reprinted with permission from ref 74. Copyright 2010 American Chemical Society. (C) Three kinds of elementary fibers packed through the hydrophobic cellulose accumulation. Reprinted with permission from ref 77. Copyright 2014 Elsevier. (D) The plant's cell wall comprises elementary cellulose fiber, lignin, and hemicellulose. Reprinted with permission from ref 93. Copyright 2014 American Society for Microbiology.

After about 20 cycles of water absorption and extrusion, the WHC of the aerogel is slightly reduced but still very impressive. Feng et al. ⁶⁷ fabricated highly porous nanocellulose aerogels from rice straw. As shown in Figure 5C–E, the aerogel density and porosity can be as low as 1.7 mg/m³ and up to 99.9%, which absorbed 210 times of water to its weight. The nanocellulose aerogels show excellent resilient properties in water and can cyclically absorb water without obvious reduction at least 4 times. To be brief, the water absorption capacity of materials mostly depends on the capillarity influenced by the porous structure of materials. Thus, by modification of the crystallinity and structure of nanocellulose materials, the distribution of FW and BW and WHC can be controlled or adjusted to meet the needs of different applications.

USING WATER VS REMOVING WATER

Using Water. Nanocellulose Hydrophilicity and Water Insolubility. Cellulose, assembled with pyranose rings via β -1,4 glycosidic bonding, has the ability to readily establish hydrogen bonds with other dipoles through the three reactive hydroxyl groups on glycoside. Therefore, cellulose is well-defined as a

hydrophilic macromolecule. As removing all water from the cellulose surface is difficult, the air-dried samples generally contain 3-10 wt % of residue water. 68 However, cellulose with superhydrophilicity is insoluble in water without assistance from high-temperature and high-pressure treatment. ^{69,70} From a biological point of view, it is rational that cellulose is insoluble in water: it serves as the primary support of plant cell walls. Additionally, a strong hydrogen bond between cellulose molecules was used to explain the dissolution of cellulose fibrils. However, a recent study indicates that hydrogen bonding between water-carbohydrate, water-water, and carbohydrate-carbohydrate interactions shows no significant difference.⁷¹ In reality, interactions between celluloses involve more than hydrogen bonding. As shown in Figure 6A, cellulose chains are linked together by hydrogen bonding to form plates. These cellulose plates tend to aggregate in order and stack into crystalline structures with lower free energy due to the van der Waals forces and hydrophobic aggregation, making cellulose insoluble. 72,73 Another important reason is the amphipathic nature of cellulose: the hydrophilic hydroxyl groups are on the equatorial plane of the cellulose chain, while the C-H in the axial direction is hydrophobic.⁷⁴ Therefore, water aggregated

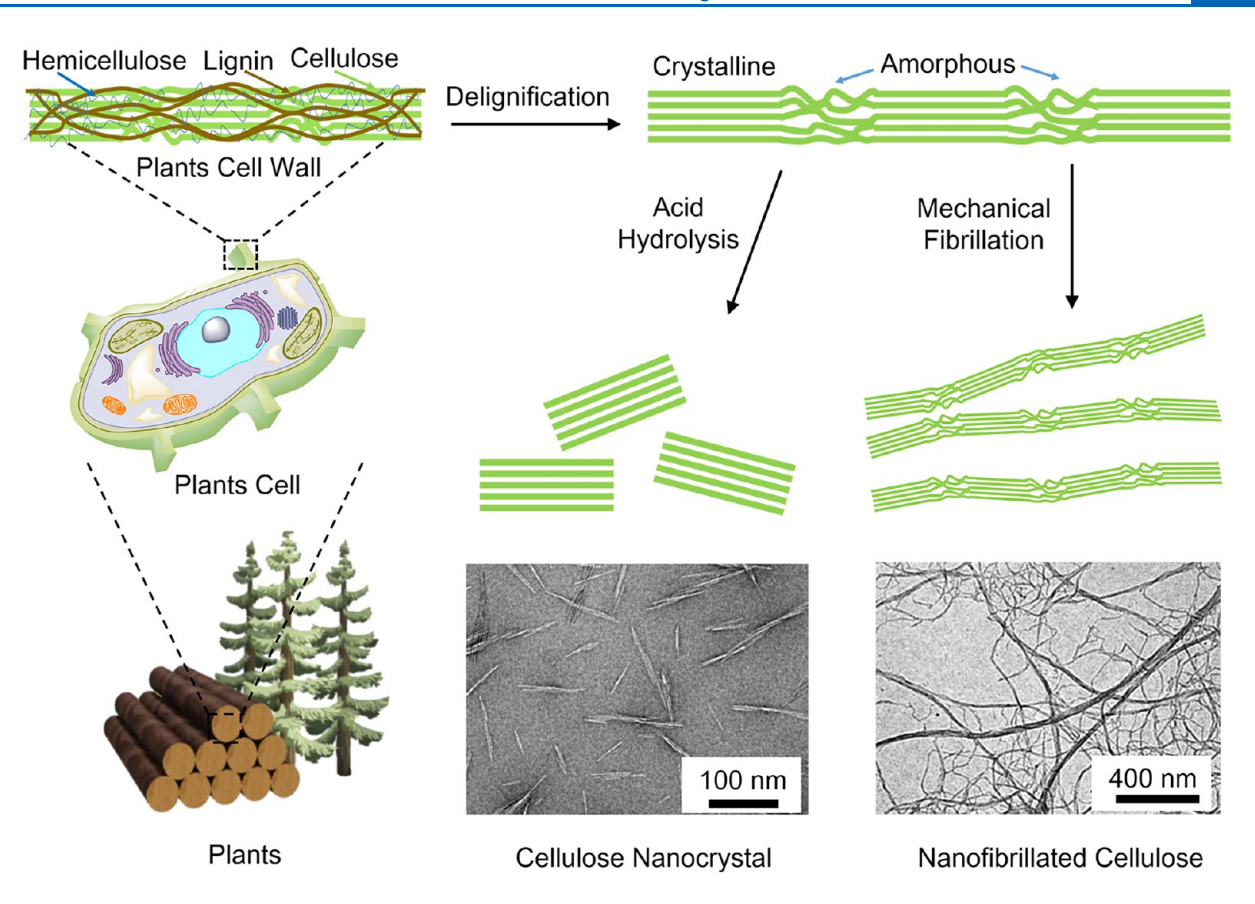


Figure 7. Schematic description of the production of nanocellulose from delignified plant cell walls with chemical- or nonchemical-assisted mechanical methods. The graphic of plants is reprinted with permission from ref 2. Copyright 2021 Springer Nature. The SEM image of CNC is reprinted with permission from ref 119. Copyright 2016 American Chemical Society. The SEM image of CNF is reprinted with permission from ref 120. Copyright 2018 Springer Nature.

around the cellulose matrix, and the formed hydrogen bond with hydroxyl groups are exposed at the side face (Figure 6B). Alternatively, water molecules tend to form hydrogen bonds with each other and stay away from the highly hydrophobic plane of the sugar ring.⁷⁵ In addition, the single-molecule experiments indicate that cellulose is somewhat hydrophobic even if the chain is molecularly dispersed in water.⁷⁶

The hydrophobic aggregation of cellulose chains has been widely recognized and accepted. It has been reported that the cellulose chains aggregate and form elementary fibrils in three modes, including 36, 24, and 18 chains shown in Figure 6C. 77,78 The elementary fibrils are the basic unit of cellulose fibril, which combines lignin and hemicellulose to make up the water-insoluble plant cell wall (Figure 6D). Although cellulose fibrils are insoluble in water, their water swelling behavior is considerable. Through sufficient water absorption, the amorphous region and crystalline surface of cellulose are well penetrated by water. Then, the increased distance between chains makes cellulose softer and more accessible to other water-soluble chemicals. In addition, metal hydroxides such as LiOH, NaOH, and KOH are more efficient swelling agents than water, making part of the crystalline cellulose swollen.⁷⁹⁻⁸¹ By disrupting the hydrogen bonding between cellulose macromolecules, a cellulose supermolecule state is formed. This state can be stabilized by introducing cooper ions as metal ligands to reconstruct the cellulose polymeric chain and open ångström-scale channels for fast ion transport.⁸² The steady coordination of copper ions inside cellulose supermolecule also benefits the facile fabrication of antiviral and antibacterial textiles.⁸³

Generally, with the increased concentration of an alkaline solution, the swelling degree will first increase and then decrease due to the relatively small hydrated ion radius of highly concentrated metal ions. Therefore, cellulose swells limitedly rather than infinitely (dissolves) in both water and metal hydroxide solvents without other assistance. A transition metal and an amine or ammonium component have been used to build cellulose solvents involving complex agents.^{84–86} However, this metal-ion-based aqueous solvent is highly undesirable due to an acid-base reaction between the cellulose and the basic metal cations, 86 which will oxidize and degrade cellulose. Alkali-based aqueous cellulose solvents, including NaOH/urea, NaOH/thiourea, and NaOH/PEG, show great promise in dissolving cellulose without degradation.8 However, the strength of the resulting products experienced a significant decrease due to the formation of cellulose II during the dissolution process. 90,91 Furthermore, the associated environmental cost, chemical usage, and equipment corrosion limit the development of water-based cellulose solvents. Instead, a more favorable approach involves fabricating cellulose I type fibrils through a disintegration process from natural cellulose, enabling the creation of mechanically robust cellulosic materials in a simple, cost-effective, and environmentally friendly manner. The pure cellulosic materials with the most impressive mechanical properties reported to date are derived from natural fiber materials, achieved by carefully

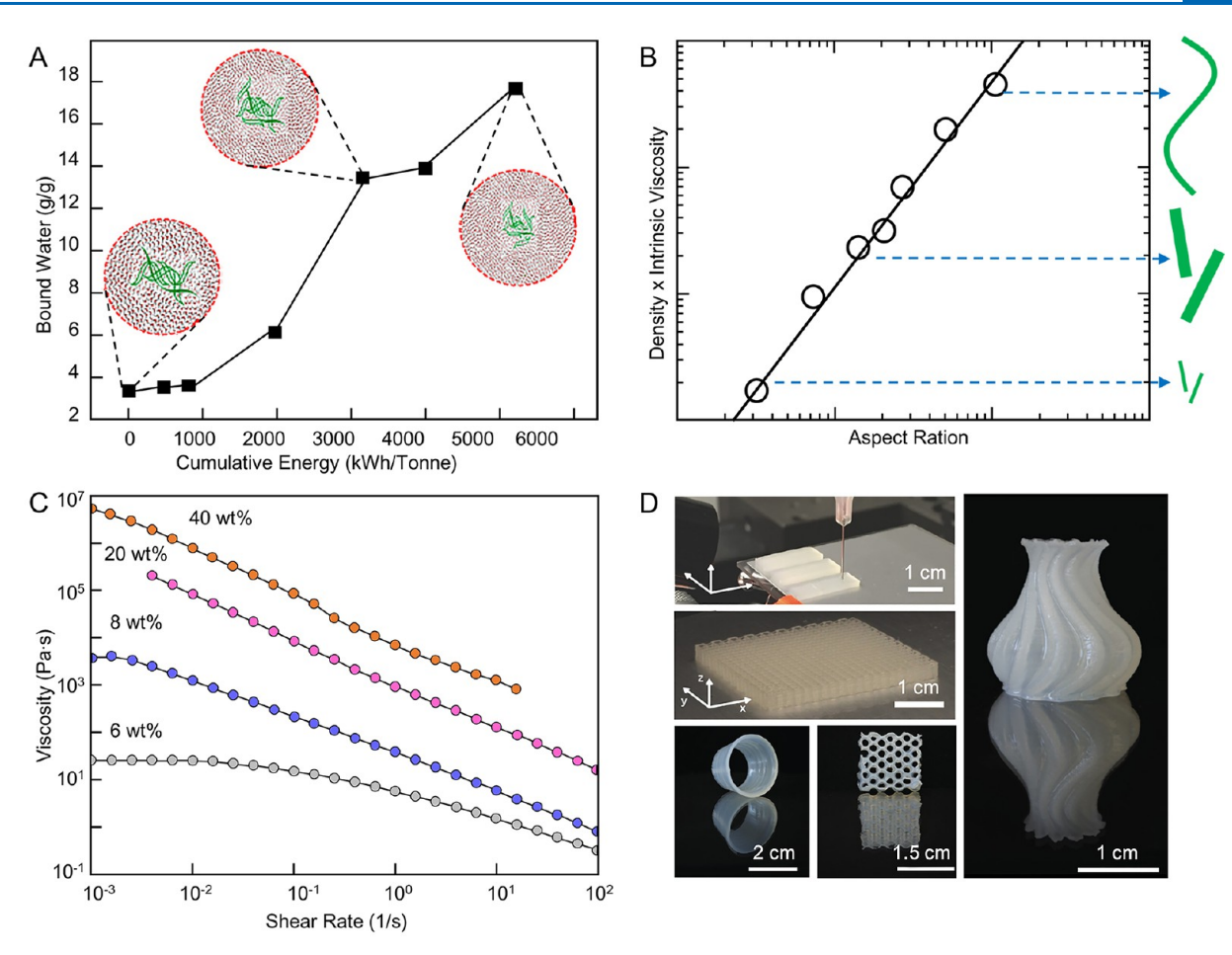


Figure 8. The rheology property of nanocellulose and its application in 3D printing. (A) Relationship among the cumulative energy, size of nanocellulose, and content of BW. Reprinted with permission from ref 121. Copyright 2020 American Chemical Society. (B) Relationship between the aspect ratio of nanocellulose and the intrinsic viscosity of the nanocellulose suspension. Reprinted with permission from ref 132. Copyright 2015 American Chemical Society. (C) The shear thinning properties of cellulose nanocrystals determined at different concentrations. Reprinted with permission from ref 133. Copyright 2017 John Wiley and Sons. (D) Images of designs from 3D-printed nanocellulose materials. Reprinted with permission from ref 134. Copyright 2019 John Wiley and Sons.

controlling water content and preserving the cellulose I type structure. As exemplified by Li et al., ⁹² cellulose I type fibrils, densely packed from naturally aligned bamboo cellulose nanofibrils, exhibit an exceptional tensile strength of 1.90 GPa, surpassing the performance of most previously reported filaments, including glass fibers and carbon nanotube fibers.

Water in Manufacturing Nanocellulose. The production of nanocellulose involves the breakdown of the multilevel structure of cellulose fibers through mechanical or chemical treatment. However, the complex multilevel structures and large size of cellulose fibers pose challenges in achieving effective dispersion and stable suspensions because more energy is required to open up the aggregation of cellulose fibrils and obtain a stable cellulose suspension. Bacterial cellulose (BC) fabrication offers a more direct way to produce nanocellulose than wood pulp because of its high purity, high aspect ratio, and nanoscale diameter (about 20-100 nm). BC fabrication tends to directly exhibit membrane and hydrogel properties instead of forming a uniform nanocellulose suspension. Therefore, the dispersion processes are necessary for producing nanocellulose suspensions that can be freely assembled to ideal materials.

The mechanical methods to make microfibrillated cellulose include high-speed shearing, ball milling, ultrafine grinding, microfluidization, homogenization, and sonication. ^{95,96} During these processes, input energy is transferred to the fluid, forming cavitation, turbulence, and shearing effects and cutting and breaking cellulose fibers into smaller fibrils. These products, made from microfibrillated processes, named microfibrillated cellulose (MFC) or nanofibrillated cellulose (NFC), retain the crystalline and amorphous regions of the original cellulose fibrils with a relatively higher aspect ratio. Therefore, MFCs are highly entangled and inherently connected fibrils with aggregated mechanically strong networks and superior hygroscopicity. ⁹⁷ The mechanical process for producing MFC is quite simple but still faces challenges, including large energy consumption and equipment clogging. ⁹⁴

Researchers are now focusing on more energy-efficient production methods by pretreating fibers with chemical and enzymatic methods. It is known that introducing charge groups will electrostatically induce the swelling of fibers as well as the hydrolysis treatment of decomposing hemicellulose or amorphous cellulose between microfibrils and elementary fibrils to facilitate the release of nanofibrils. Therefore, chemical and enzymatic pretreatments decrease fiber cohesion and alleviate energy consumption during delamination. Previously, reports have demonstrated TEMPO-oxidation, carboxymethylation, and enzymatic treatment as successful

pretreatments to produce CNF suspensions with higher hygroscopicity and superior rheology. 97-101 In addition, several emerging technologies, including phosphorylation, sulfonation, periodate-chlorite oxidation, cationization, and carboxymethyl cellulose grafting, have been tested to provide CNF suspensions, for their potential to introduce charge groups on cellulose and accelerate the swelling and nanonization of cellulose fibril. 96,102-105 Through chemical and biochemical treatment, CNF exhibits a soft and long chain of widths ranging from 10 to 100 nm and lengths ranging from a few hundred nanometers to micrometers (Figure 7). Other typical cellulose I nanofibrils are cellulose nanocrystals (CNC) formed from acid hydrolysis and oxidation. The amorphous region of cellulose fibrils is selectively degraded during hydrolysis and leaves isolated highly crystalline nanowhiskers. In addition, a negative surface charge usually comes up with acid treatment, which facilitates the dispersion of CNC and induces a stable CNC colloid in water. Sulfuric acid and other acids were investigated, including hydrochloric, hydrobromic, citric, phosphoric, oxalic, and maleic acids, to produce CNC. 96,106–110 In brief, CNF and CNC production methods are related to the chemical reaction on the surface hydroxyl groups of cellulose in water, which either actively or passively causes these materials to become highly hydrophilic. Therefore, the production of CNF and CNC highly relies on water, which plays a vital role as a solvent for chemical reactions and nanocellulose dispersions.

Recently, aliphatic esters, rather than hydrophilic ionic surface groups, were introduced on the cellulose surface to fabricate cellulose nanofibers with hydrophobicity and water stability. 111-114 These modifications required dried cellulose and organic solvents as reaction media to generate cellulose with poor processability in water, bringing forth concerns about its environment and cost. However, Beaumont et al. 115,116 found that the existence of water benefits the regioselective esterification of cellulose, and esterified CNF was fibrillated and suspended in water with fluid properties similar to those of CNF. Furthermore, the esterification of cellulose can be reversed by modifying functional groups on its surface, enabling facile aqueous processing after esterification and impressive recovery of natural nanocellulose performance after ester hydrolysis. 117 They also found that the waterassisted surface functionalization of cellulose could come up in humid environments, which induced surface-confined water (bound water) as a reaction medium. 118

Rheology Properties and 3D Printing. Cellulose fibril morphology and size changes will induce different degrees of exposure to hydroxyl groups and thus influence the rheological properties of fluids. More water will be absorbed on the cellulose surface with smaller diameters and larger aspect ratios due to the hydroxyl groups on the equatorial planes of the cellulose chain. As shown in Figure 8A, it has been reported that the size of nanocellulose will decrease with increasing output energy of mechanical disruption while the content of bound water increases. 121 Therefore, a cellulose suspension is usually diluted before microfluidization to fabricate nanocellulose fibers with nanoscale size. 122 Nanocelluloses with larger aspect ratios show an increasing attraction of BW, which is positively related to the density multiplied by the intrinsic viscosity of the cellulose suspension, as shown in Figure 8B. In other words, nanocellulose fibrils entangle more than cellulose fibers with the same concentration. Therefore, nanocellulose can only be isolated without entanglement when the

suspension concentration is low enough. Isogai et al. 122 measured the boundary concentration of TEMPO-oxidized nanocellulose between dilute and semidilute regions. They reported that the nanocellulose solution with a concentration lower than 0.12% w/v was the diluted dispersion that could be used to evaluate the length of nanofibers. With the increasing concentration of cellulose suspension, cellulose entangles and aggregates because there is insufficient FW to separate the fibrils. During the concentration process, the cellulose suspension transfers from dilute to semidilute and from semidilute to gel solution with increasing viscosity. In addition, the size and aspect ratio of fibers are closely related to the gelation of cellulose suspension, because the intrinsic reason for gelation is hydrogen bonding between cellulose. It has been reported that the gelation concentration of a nanocellulose suspension increased 4 times while the aspect ratio of nanocellulose was reduced to half of what it was. 123 Furthermore, the solution showed excellent rheological properties when the concentration of nanocellulose was higher than 20 wt % (Figure 8C).

The combined interactions between cellulose and water give the cellulose suspension excellent shear-thinning rheological properties and gelation behavior above the critical concentration. These capabilities make nanocellulose-water suspensions a biocompatible, low-cost, and fascinating material, serving as a building block, filler, matrix, and rheological modifier in 3D printing. Gelation behavior originating from entanglements of nanocellulose in water allows nanocellulose to construct self-standing structures by 3D printing, which permits the rebuilding of various fancy structures, as shown in Figure 8D. With almost zero toxicity and genotoxicity against cells, nanocellulose is considered a good supporter of tissue engineering through 3D printing. 124 Furthermore, thanks to the superior rheological properties and amphipathicity, nanocellulose can be utilized as a surfactant for dispersing CNT, 125,126 lithium metal, 127 graphene oxide, 127 graphite, 12 carbon black, 128 and boron nitride. 129 Therefore, nanocellulose slurries with printable properties enable accurate reconstruction of materials applicable in energy storage, solar steam devices, water harvesting, and thermally stable ion conductive materials. As a mechanically robust material, nanocellulose was used as a filler to reinforce materials and humidity responses in the soft matrix. 130 However, using nanocellulose in 3D printing is not ideal, as the resolution ratio and structure stability of building blocks are sensitive to the drying process and environmental humidity. Different cross-linking methods, such as ion and covalent bond cross-linking, were considered to keep the shape from collapsing. 131 Thus, critical issues still need to be considered to stabilize the structure, enhance printing resolution, and control the humidity sensitivity of nanocellulose-based 3D printing materials.

Rehydration and Reformation of Nanocellulose. Due to the inherent hydrophilicity of nanocellulose, water can readily permeate the material and establish bonds with the hydroxyl groups present. Compared to the hydroxyl groups confined within the cellulose macromolecule and influenced by its configuration, water molecules, functioning as both hydrogen bond acceptors and donors, exhibit greater flexibility. They tend to organize into water clusters and create hydrogen bonding networks encompassing water—water and water—cellulose interactions. Consequently, the cellulosic fibrils undergo swelling, and water assumes the role of a plasticizer, lowering the material glass transition temperature, rendering it

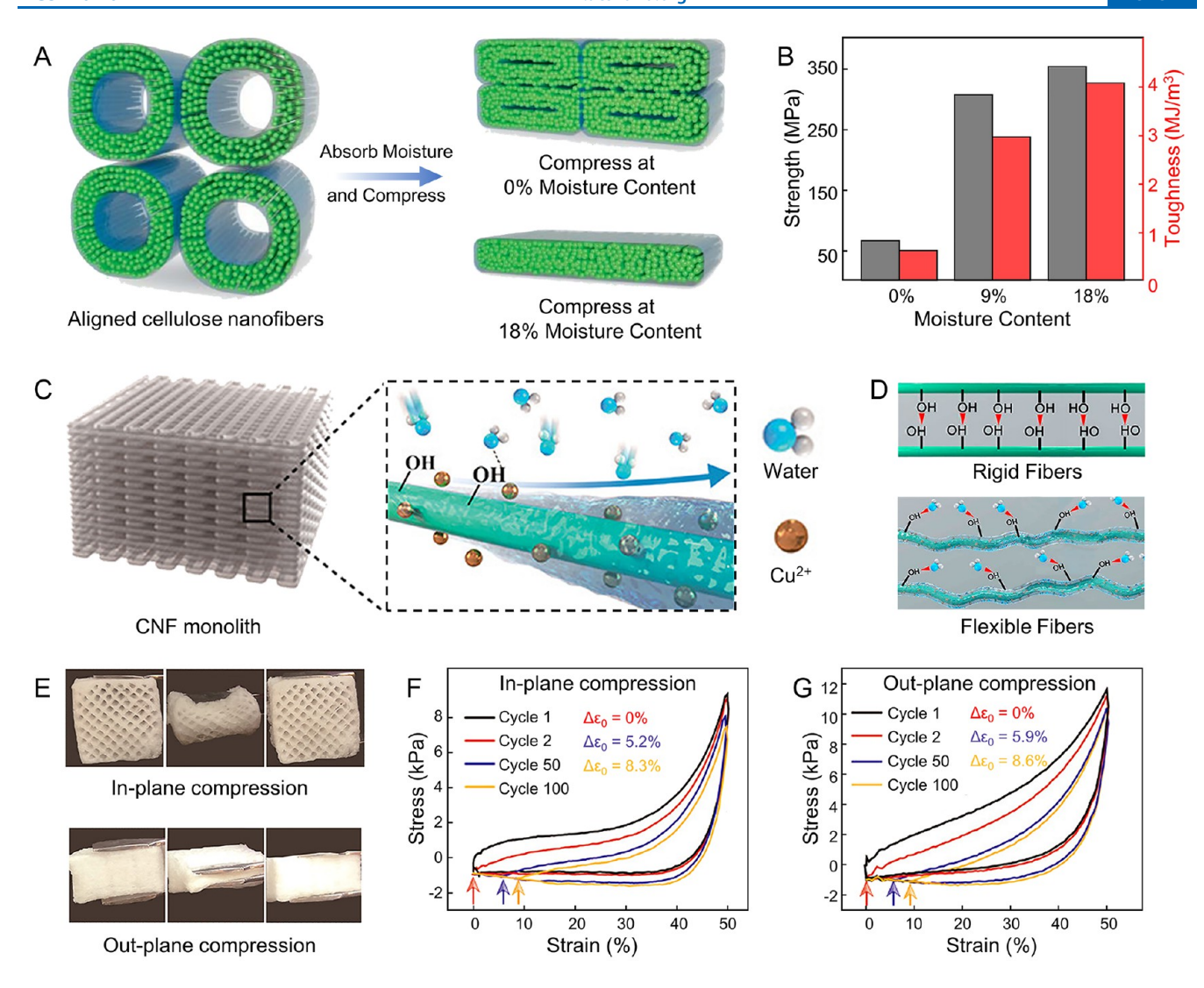


Figure 9. Water as a plasticizer to soften materials and assist deformation. (A, B) Schematic illustration (A) of the better compressibility of cellulose nanofiber bulk materials with higher moisture content and (B) mechanical properties of compressed cellulose nanofiber bulk materials at varied moisture content. Reprinted with permission from ref 138. Copyright 2019 Royal Society of Chemistry. (C–G) Illustrations of CaCl₂-induced cross-linking and water adsorption in CNF monolith (C) and water molecules activated shape recovery properties of cellulose fibers (D). Shape recovery properties of the CNF monolith om in-plane (E, F) and out-of-plane compression (E, G). Reprinted with permission from ref 140. Copyright 2021 American Chemical Society.

more pliable and facilitating deformation. Water significantly enhances flexibility, even in the presence of only a small amount of moisture within the material. BW, in particular, has been observed to contribute positively to the deformation^{5,135} and mechanical properties^{136–138} of cellulosic materials. As illustrated in Figure 9A,B, Han et al.¹³⁸ rehydrated delignified wood, allowing water to penetrate cellulose nanofibers and establish additional hydrogen bonds. Subsequent compression tests demonstrated that the density and mechanical strength of the compressed wood exhibited a direct correlation with the increasing content of BW. BW serves as a structural element within the network, bridging cellulose nanofibers and facilitating the interaction between wood cells and nanocellulose. Water molecules soften the materials during rehydration and promote easier material reformation during dehydration (compression). As reported by Han et al., 136 an appropriate amount of water in dried wood aerogels fosters the formation of additional hydrogen bonds among cellulose

nanofibers, making the wood more amenable to compression and resulting in stronger materials.

When nanocellulose materials become fully saturated with water, this has a beneficial effect on the shape recovery of these cellulosic materials. By strategically designing nanocellulose materials with wet resilience, we can permeate every pore within the materials without causing them to collapse. Upon full saturation in water, the FW within the hydrogen bond network can swiftly exchange with water in the surrounding solution. Meanwhile, BW acts as a supportive bridge between nanocellulose components, providing a soft support to the materials. In this case, with insufficient compression that does not collapse the micro- or nanopores within the materials, the water within the materials can readily respond to deformation and facilitate shape recovery. Jiang et al. 67,139 demonstrated that CNF aerogels produced by freeze-drying exhibited wet resilience and shape recoverability when subjected to compression of less than 60% in an aqueous environment. The excellent shape recovery attributes are attributed to

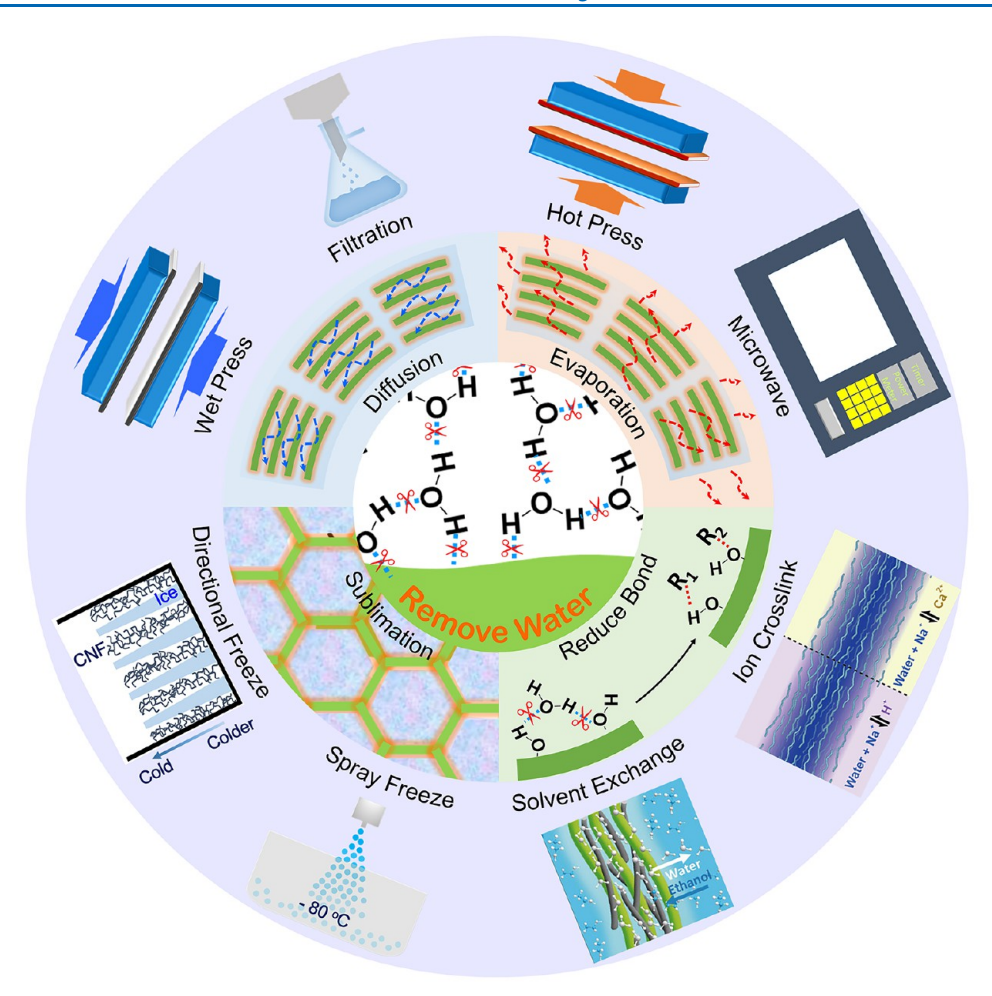


Figure 10. Schematic description of methods for removing water from nanocellulose materials through diffusion (e.g., filtration and wet press), evaporation (e.g., hot press and microwave), and sublimation (e.g., directional and spray freeze) of water, and reduction of cellulose—water hydrogen bonds (e.g., solvent exchange and ion cross-linking). Sample of directional freeze-drying is reprinted with permission from ref 178. Copyright 2019 Springer Nature. Sample of solvent exchange is reprinted with permission from ref 179. Copyright 2017 John Wiley and Sons. Sample of ion cross-linking is reprinted with permission under Creative Commons Attribution 4.0 International License (https://creativecommons.org/licenses/by/4.0/) from ref 180. Copyright 2019 Springer Nature.

limited compression and a hydrogen bonding network capable of rapid dynamic changes. Water plays a critical role in mediating the flexibility of nanocellulose materials through processes such as soaking and humidity control.

Nevertheless, controlling water content via soaking can be challenging, and humidity-based methods for water content control are influenced by the inherent structure and hygroscopic properties of the material, rendering them sensitive to environmental conditions. In a different approach, Chen et al. He employed a hygroscopic salt (CaCl₂) to regulate water absorption in CNF monoliths (as illustrated in Figure 9C–G). This treatment significantly increased the water uptake of nanocellulose materials at room temperature and humidity (25 °C and 43% RH), elevating it from 8% to approximately 75%. Consequently, a transition from rigidity to elasticity in nanocellulose materials was observed, with water acting as a plasticizer that enhanced the material shape recovery capability by a factor of 100 under room-temperature and -humidity conditions.

Removing Water. *Motion of Water and Cellulose.* Thanks to the inherent hydrophilicity of cellulose, cellulose fibers could be permeated by water and form nanocellulose suspensions in an environmentally friendly and cost-effective

manner. However, water needs to be removed from the nanocellulose suspension to manufacture biodegradable and mechanically strong films, fibers, and foams through various drying methods with exceptions for building hydrogel materials or modified inks in 3D printing. During the drying process, the intermolecular forces of cellulose and water play a significant role and give water three states according to their mobility: FW, LBW, and TBW. Removing water from a nanocellulose suspension generally involves breaking the interaction between cellulose and water. From this viewpoint, dewatering methods, as shown in Figure 10, can be clarified into two major parts: activating the movement of water and reducing the bonding between cellulose and water. Table 2 provides an overview of conventional approaches for water removal by triggering water movement.

Activating Water—Liquid to Liquid. Generally, liquid water can be removed from a nanocellulose suspension by applying force (e.g., shear, press) to the suspension, inducing the separation between water and cellulose. In this process, the major type of water capable of traversing through channels in the nanocellulose network is FW with high mobility, while a substantial number of BW remains within the nanocellulose slurry. This partial water removal, called dewatering, involves

Table 2. Conventional Dewatering and Drying Method to Remove Water from Nanocellulose Materials

methods	input and output materials	water removal efficiency	material structural characteristics
filtration	suspension to gel-like cake	FW is removed in hours	gravity and/or pressure drive FW removal and solid content increase
shearing	gel	auxiliary dewatering of FW	internal stress induces fibril entanglement and phase separation to form a flocculated gel
pressing	wet mat	FW and partial LBW are removed in hours	compression induces drainage and drives densification
air-drying	CNF slurry	FW and partial LBW are removed in hours, with no energy input	
oven-drying	suspension/gel to bulk material	FW and partial BW are removed in hours	capillary and diffusion forces drive densification
hot-pressing	gel/mat to bulk material	FW and partial BW are removed in hours	capitally and distaston forces after designed on
microwave	suspension/gel/mat to bulk material	FW and partial BW are removed in minutes, with high energy efficiency	
spray-drying	suspension to powder	FW and partial BW are removed in hours	atomization reduces the size to form small droplets
			capillary and diffusion forces drive densification to form microand nanoparticles
freeze-drying	suspension/gel/mat to powder or porous materials	FW and partial FBW are removed in days.	ice growth induces fibril agglomeration and the formation of 2D-sheet inner walls
			ice sublimation forms a porous structure
spray freeze- drying	suspension to powder or aerogel	FW and partial FBW are removed in days	atomization reduces the size to form small droplets
			restricted ice growth induces less fibril agglomeration and the formation of a filamentous inner wall
			ice sublimation forms a porous structure
supercritical drying	suspension/gel/mat to powder or porous materials	FW and partial BW are removed in hours	solvent exchange
			suppressed capillary force induces less fibril agglomeration and the formation of filamentous inner walls
			Gasification of CO ₂ forms a porous structure.

various methods, including filtration, shear stress, and wet pressing. Filtration processing is commonly employed for dewatering nanocellulose on a lab scale, but it typically requires several hours due to the high water retention properties of nanocellulose. 141 As reported by Rol et al., 142 filtering a 2 wt % CNF suspension by gravity and aspiration proved ineffective in increasing the solid content, because of the viscous and gel-like behavior of CNF. A large number of water molecules remained trapped within the nanocellulose network, resisting extraction by a vacuum force. Although filtration cannot completely remove water from the materials, it is the simplest and most cost-effective method for removing predominant FW. Moreover, vacuum filtration is a facile approach for fabricating sandwich-like nanocellulose composite membranes applied in sustainable energy storage systems. 143 The shear stress method usually works as an auxiliary to the filtration method due to its low efficiency. For example, the relationship between dewatering and rheological behavior was investigated by Dimic-Misic. 141,144-147 They found that ultralow shear might cause phase separation and dewatering in the nanocellulose solution, speeding up the vacuum filtration. 141,144-147 Wet pressing is another standard method for MFC dewatering; it could compress the nanocellulose suspension with a plate and frame, resulting in a compressed pad with 18 wt %. 141 To summarize, these three dewatering methods are recognized

through capillary percolation by forcing the suspension through mechanical, shear, and atmospheric pressure. These processes mainly remove the FW, which barely interacts with cellulose and has the best motility in the solution, leaving a wet gel/mat rather than a dried film or web. The assistance of evaporation or sublimation of water is required to achieve complete dewatering of nanocellulose.

Activating Water—Liquid to Gas. The nanocellulose materials can be dried thoroughly with air and heat by transforming the FW and LBW from liquid to gas. TBW and partially LBW would remain in the material because of rewetting in the air. It is easy to accomplish air-drying by placing the moist material in the dry air. The humidity differences and Brownian motion of molecules will induce the release of water molecules from moist materials into the air. Finally, the water content in materials comes to balance with the relative humidity of air (Figure 5A). Air drying is energy-efficient with nearly zero energy consumption. However, it generally takes a long time due to the slow water evaporation process occurring under ambient conditions and is restricted by environmental humidity.

The water evaporation can be sped up through the heating process by absorbing energy from heat sources. In this process, the nanocellulose suspension absorbs energy, reaching a high temperature where the nanocellulose remains stable while

Table 3. Water Removal Methods Applied to Nanocellulose Materials for Reducing Water-Cellulose Hydrogen Bonding

materials	methods	dehydration mechanism	mechanical properties	application	references
CNF nanopaper	vacuum filtration lactic acid modified hot pressing	lactic acid modified hydroxyl groups and improved hydrophobization of nanofibers	tensile strength (~170 MPa)	higher CNF content and faster drainage	169
porous cnf nanopaper	vacuum filtration SE (hexane)	filtration-based solvent exchange suppressed the aggregation of nanofiber		transparent and air-permeable nanopaper	165
holocellulose nanofibril film	vacuum filtration SE (ethanol, hexane) AD	hexane evaporation enhanced inter-HCNFs hydrogen bonding interactions	tensile strength (84.8 MPa)	high-haze transparent holocellulose nanofibril film	166
CNF/CNT foam	FC SE (ethanol) AD	FC induced aligned growth of cell walls Low surface tension of ethanol stabilized the microstructure during AD	compression module (85.9 kPa)	electromagnetic interference shielding	167
CNF/pulp foam	vacuum filtration SE (ethanol) AD	low surface tension of ethanol prevented uneven shrinking within the foam	compression modulus (0.49–2.96 MPa)	low cost, practicable, and scalable	168
CNF/alginate aerogels	IC (NaCl, CaCl ₂) SE (ethanol, hexane)	ions decreased the electrostatic repulsion between nanofibers	compression modulus (97–275 kPa)	energy storage, mechanical strain, and humidity sensors	171
CNF xerogel	IC (Al ³⁺) SE (ethanol, hexane) AD	Al³+ cross-linking induced self-standing, stiff gel	compression modulus (170 MPa) tensile strength (8 MPa)	light permeability, thermal insulation, and flame self-extinction	172

water undergoes a phase change from liquid to gas. Based on the heating type, heat drying processes can be clarified into two types: thermal transfer methods (oven heat, hot-plate heat, hot press, and spray-drying) and dielectric heating methods (microwave). In a laboratory setting, oven and hot-plate heating are commonly used drying techniques, allowing rapid, convenient, and shape-unrestricted drying of the moist nanocellulose. On the other hand, hot pressing can effectively densify materials and prevent curling by applying high pressure during the drying process, especially in the longitudinal direction. In other words, hot pressing builds nanocellulose films with enhanced density and strength compared with the outcomes of oven and hot-plate heating. Furthermore, the selfassembly behavior of nanocellulose during drying plays a crucial role in determining the morphology of the nanocellulose-based materials. For instance, CNC, characterized by self-twisted and parallelepiped structures, can pack together and form a liquid crystalline phase at specific concentrations. By programming of the drying process, CNC suspensions can be dried into colored films. Although limited research has focused on the CNC-water interaction, it is believed to be a pivotal factor in mediating self-assembly behavior during the construction of nanocellulose materials. 149

Another efficient thermal transfer method is spray-drying, which can cause ultrafast drying of nanocellulose materials by spraying them into small particles to increase the thermal conversion area. The morphology and size of these nanocellulose particles are influenced by gas velocity, liquid input, and the concentration of nanocellulose. 150 As for the dielectric heating methods, microwave heating has been used in drying wood and bamboo with fast and uniform heating, leading to very different products with low porosity. 151-153 Up to now, only a few reports have applied microwave heating in drying nanocellulose materials. For example, Rol et al. 142 produced nanocellulose objects through cellulose molding processes and examined various drying strategies, covering thermo-pressing, oven, microwave, and freeze-drying. Although microwaves could dehydrate materials in 5 min, it was found that the water vapor generated during the microwave would damage the cellulose mold and mat, create pores inside the material, and easily cause hornification and degradation of cellulose.

In this evaporation process induced by humidity difference and heating, water can be released from materials by breaking the water—nanocellulose hydrogen bonding with a sufficient time or energy supply. During this process, FW and most of the BW in nanocellulose materials is removed, and numerous cellulose—cellulose hydrogen bonds will be generated to give high strength to the nanocellulose materials. 148

Activating Water—Solid to Gas. Another effective method for removing water is freeze-drying, which transfers water from the solid to gas. In this process, water freezes into ice and then sublimates in a vacuum. FW and FBW will freeze and form ice crystals, while NFBW remains bonded to the hydroxyl group. Therefore, the freeze-drying process involves the primary drying stage, which sublimes ice of freezable water, and the secondary drying stage, which evaporates NFBW under a vacuum. 154 Unlike the heating process, capillary force and surface tension are minimized in the freeze-drying process, resulting in a porous dried nanocellulose material. ¹⁵⁵ Owing to the separation of ice crystal and nanocellulose, nanocellulose will aggregate in the gap between ice crystals and form 2Dsheet inner walls. 156 After sublimation, ice crystals are removed, leaving pores in the material. Thus, the freeze-drying method is widely applied in constructing cellulose-based 3D porous materials. The water content, nanocellulose morphology, freezing temperature, and direction control the distribution and morphology of pores.

Nanocellulose aerogels built by freeze-drying are characterized by low density and high porosity and thus have a high specific surface area. The high content of hydroxyl groups on the surface of nanocellulose and the high specific surface area of the aerogel can efficiently absorb dyes, metals, and gases. It can be used in wastewater and waste gas treatment, oil spillage, and electromagnetic shielding. Directional freezing allows the ice to grow from the near side of the cold source to the far side, creating aligned pore structures in the nanocellulose aerogel. After constructing the aligned pores, anisotropic nanocellulose aerogels become highly compressible and are applied in various advanced devices, including oil absorption, ¹⁵⁹ energy storage, ¹⁴³, ¹⁶⁰ and thermal insulation. ¹⁶¹ Jiang's group ^{162–164} has made outstanding progress in the preparation and application of anisotropic aerogels fabricated by directional freezing. Since the directional growth of ice crystals is affected by heat transfer, the growth process shows a gradient, and most of the reported directional growth materials show partial structural anisotropy or an "inverted trapezoid" structure. 162 Chen et al. 162 dropped the mold into the freezing liquid at a slow speed, and the external velocity and ice crystal growth driving force worked together to balance the ice crystal growth and achieve the preparation of ultralong anisotropic aerogels. Thanks to the rapid transport of dye and solvent molecules through directional pores, 163 this ultralong anisotropic structure can transport liquids and achieve real-time water purification. By incorporating silver nanowire and Fe₃O₄, the anisotropic nanocellulose sponge yields better electromagnetic interference shielding performance in the transverse direction compared to commercial standards. 164

Spray-freeze-drying, a less frequently mentioned method, is also applied as a sublimation drying method. Similar to spray drying, spray-freezing sprays the materials into small particles at first. Then, these small particles exchange thermally with the heat source and freeze for sublimation in a short time. Jiménez-Saelices et al. 156 manufactured a nanocellulose aerogel with thermal superinsulating properties by spray-freeze-drying. They discovered that the spray-freeze-drying process, which involves rapid cooling of the droplets, effectively limits ice crystal growth and results in aerogels featuring a three-dimensional fibril skeleton morphology.

Decreasing the Bonding between Water and Cellulose. As previously stated, a key step in water removal involves disrupting the contact between cellulose and water. To achieve this, various methods, such as solvent exchange (SE), ion cross-linking (IC), hydrophobic modification, freeze crosslinking (FC), and additive absorption, have been employed to diminish water-cellulose hydrogen bonding, facilitate rapid drainage, and enable ambient drying (AD). Table 3 provides several examples of the application of these techniques. The effectiveness of drying procedures, including air-drying and heat-drying, can be improved by substituting low-boiling solvents, including ethanol, acetone, and hexane, for FW and a part of BW. This substitution not only accelerates the drying speed but also leads to reduced energy consumption, thus resulting in cost savings. For example, Huang et al. 165 applied ethanol and hexane to exchange water in a nanocellulose suspension before filtration, allowing the fabrication of transparent and air-permeable nanopaper by fast filtration and ambient drying. Han et al. 166 applied hexane in SE drying of manau rattan originated nanocellulose, and they found that SE slightly increased the mechanical properties of nanocellulose films compared to air-dried films. Zeng et al. 167 immersed frozen CNT/nanocellulose hydrogel in ethanol and then dried the sample at 80 °C for 0.5 h, at 170 °C for 15 min, and at room temperature overnight. Additionally, SE with ethanol was found to prevent uneven shrinkage within the foam, promoting the material to maintain a stable structure in ambient drying. 168 Supercritical drying can be used for drying nanocellulose by replacing ethanol with CO₂. In this method, ethanol replaces water before drying because cellulose will be destroyed at the critical point of water (374 °C, 229 bar) since water and CO2 are immiscible. A filamentous skeleton can be obtained due to the suppressed capillary force and aggregation of nanocellulose in the gasification of CO₂. However, high energy, chemical, and equipment costs limit the development of supercritical CO₂ drying in nanocellulose material

Another practical approach for removing water is reducing water-cellulose hydrogen bonding by additives that can attract nanocellulose or compress the hydration layer. This method inhibits BW from forming in the system and converted into FW, so the water can be removed more easily. For example, Amini et al.²⁹ reported "contact dewatering", where the majority of the absorbed water would be converted to FW through the interaction of wood particles with nanocellulose, enhancing the dewatering efficiency. Sethi et al. 169 found that adding lactic acid would decrease the drainage time from 45 to 29 min without heating and sonication. Sim et al. 170 discovered that nanocellulose could absorb cations, such as Na⁺ and Ca²⁺, resulting in the electrical double-layer compression, nanocellulose aggregation, and acceleration of the dehydration. Salts are more commonly reported in cross-linking nanocellulose to assist the formation of a stiff and stable nanocellulose skeleton in conjunction with FC and SE to achieve porous materials enabling AD. Françon et al. 171 applied FC, IC, and SE to fabricate wet stable aerogels, allowing for their subsequent drying under ambient conditions. They observed that cations decreased the electrostatic repulsion between nanofibers and helped keep nanocellulose/alginate foam from shrinking in AD. Sakuma et al. 172 applied Al 3+ cross-linking and FC to form a self-standing and stiff gel and dried the gel under ambient conditions by SE with ethanol and hexane. Thanks to the amphipathicity of nanocellulose, adding hydrophobic substances such as graphite in the suspension can also cause the aggregation of nanocellulose and promote the dehydration. Assisted by IC and a foaming agent (SDS), graphite—nanocellulose foam can form a stable structure and be dried under ambient conditions without SE. ¹⁷³ Interestingly, the synergistic effect between graphite and Cu²⁺ during combustion endows Cu²⁺ ionically cross-linked graphite—nanocellulose with excellent fire resistance. ¹⁷⁴ In addition to graphite, it has been reported that the coordination interaction between nanocellulose and bentonite can also be used to create a strong building block. ¹⁷⁵ By freezing, nanocellulose and bentonite further aggregated to form a strong and stable inner structure, thereby achieving this without SE. ¹⁷⁶

Traditional drying methods, relying on the phase transition of water, are straightforward but come with high energy consumption due to strong hydrogen bonding and the high transition enthalpy of water. Additionally, the substantial water requirement to prevent nanocellulose entanglement during processing while ensuring material uniformity necessitates efficient and cost-effective drying methods. Therefore, the prospect of combining strategies to decrease cellulose-water bonding with the phase transition of water holds promise for concurrently reducing both time and energy costs. For the drying methods based on the phase transition of water, cellulose molecules become close to each other, tangle, and build more cellulose-cellulose hydrogen bonds, due to the capillary and diffusion force and the freezing-induced crosslink. As a result, the stable hydrogen bonds make the fibers challenging to separate, leading to cellulose aggregation, entanglement, and even hornification. Although the entanglement and aggregation would densify the material into a more stable structure, from the view of industrial-scale production, avoiding the aggregation and hornification of fibers after dehydration and improving the redispersibility of fibers is of great value in reducing storage and transportation costs and realizing the large-scale production and application of nanocellulose. Surface charge modification, steric hindrance enhancement, solvent exchanging, and controlled drying processes have been studied to improve the nanocellulose redispersibility, based on preventing the formation of cellulose-cellulose hydrogen bonds. 17

Depending on the method employed, the drying process can modulate the type of interactions among cellulose fibers, consequently influencing the overall structure and properties of the cellulosic material. Conventional heating methods such as oven-drying and hot pressing could form dense and strong 1D and 2D materials, due to the water molecule bridging and the capillary and diffusion force inducing the forming of nanocellulose intermolecular hydrogen bonds. Freezing methods could form 3D porous materials with filamentous or 2D-sheet inner walls by controlling ice growth. Ion cross-linking and interaction between nanocellulose and 2D materials/polymers improve the dewatering efficiency and negatively impact material molding. However, they significantly affect the structure, strength, and functionalization of materials.

EXCESS WATER VS LACKING WATER

Influence of Water on Processing. The production of nanocellulose-based materials heavily relies on water due to the hydrophilicity of cellulose molecules and the versatile use of water. Water plays a critical role in swelling and dispersing nanofibers, assembling and softening nanofibers, transferring chemicals and heat, and transporting and storing nanocellulose.

During the nanocellulose production process, achieving homogenization of the cellulose fibril is controlled not only by the surface functionalization of cellulose but also by the water content in the suspension. With enough water, fibers can fully swell, soften, and isolate from each other, ready for fibrillation into nanocellulose. Producing nanocellulose by high-pressure homogenization is promoted by the high mechanical shearing forces, the rapid pressure drop, the turbulent flow, and the frictional forces of the particles against each other. 181,182 The excess water would weaken the friction between fibers, reduce the nanocellulose yield, and increase undesirable energy costs and water consumption. Under conditions that lack water, the feedstock will aggregate and block nozzles to reduce the efficiency and lifetime of the equipment. Due to the clog-free machine design, the grinding methods were reported to be capable of grinding a fiber-water suspension with a concentration of up to 2-5% w/v. 181

With enough water, evaporation and crystallization of water would assemble nanocellulose by capillary force and ice squeezing, enabling densified and porous bulk materials. In addition, water flow could assist the assembly of nanocellulose into filaments. Söderberg et al. 183,184 applied a flow-focusing method to the assembly of nanocellulose, aligned it with the flow direction, and yielded a mechanically strong filament with a tensile strength of 1.57 GPa. Excess water would isolate nanocellulose, inhibit fiber-to-fiber contact, and induce uneven and powdered products. Lack of water will lead to poor fiber fluidity and an uneven internal system, making it difficult to shape the material and control its structure. For nanocellulose materials that have been dried, the appropriate rehydration can soften the nanofibers and promote the deformation of the material. The lack of water can cause structure collapse during deformation, while excess water can break down fibrous materials such as paper that are not sufficiently cross-linked.

Water also plays an essential role in transferring chemicals and heat as well as transporting and storing nanocellulose in the cellulose industry. Adequate moisture can promote the uniform penetration transfer and distribution of chemicals and heat in the fiber network during various chemical processes, such as delignification and TEMPO oxidation, allowing reactions to occur evenly. The lack of water will lead to uneven reactions and reduced product yield and quality, while excessive water will dilute the medicinal solution, increase energy consumption, and reduce the product yield and quality as well. In the transportation and storage of nanocellulose, water can suppress the excessive aggregation of nanocellulose and benefit the following material production.

Influence of Water on the Mechanical Properties. The excellent mechanical properties of the nanocellulose material are generally attributed to inherent strength. Cellulose elementary fibrils show extraordinary mechanical properties throughout the crystalline region. The elastic modulus of the crystalline region in nanocellulose, estimated by X-ray diffraction and Raman microscopy in the axial direction, falls within a range from 130 to 250 GPa, comparable to that of glass fibers. 185-188 However, the nanocellulose material comprises several elementary fibrils or microfibrils with crystalline and amorphous regions. Hence, the natural amorphous region, constitutive structure, intermolecular hydrogen bonding, van der Waals force, and friction force also affect the mechanical properties of nanocellulose materials. Pure crystalline celluloses such as MCC and CNC made from sulfuric acid treatments exhibit excellent strength but are

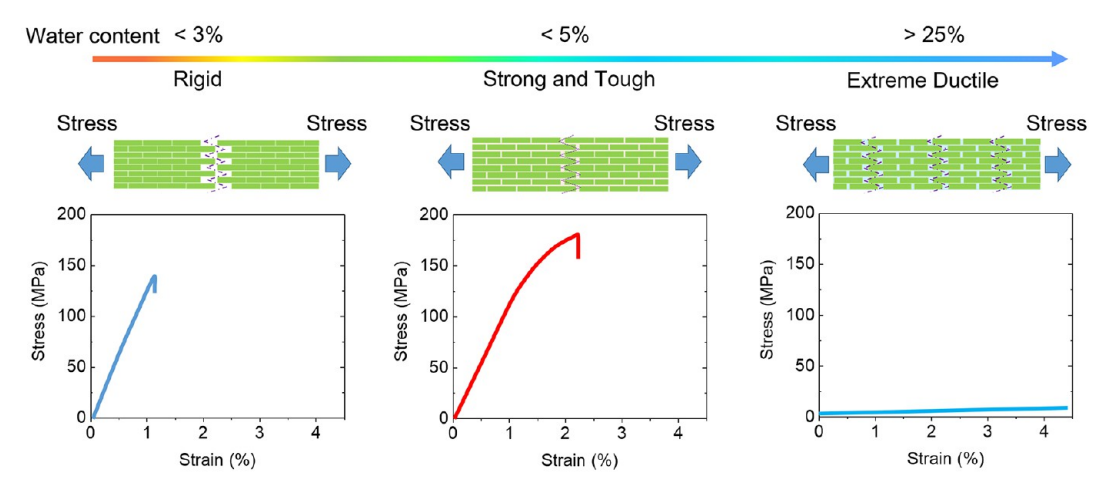


Figure 11. Schematic description of the mechanical properties of cellulosic materials with different water content. The strain-stress diagrams and the schematic stretching model were redesigned with permission from ref 196. Copyright 2021 American Chemical Society.

inferior to the CNF and BC due to the lower aspect ratio and specific area.¹⁸⁹ Packing cellulose on the nanoscale will reduce the number of pores and defects in materials and increase the strength. For example, the cellulosic materials made from aligned and compact nanocellulose show modulus and strength values higher than 60 and 1 GPa.¹⁸³

Due to the moisture sensitivity of hydroxyl groups and the complicated constitution of the source of strength, the mechanical properties of nanocellulose materials are sensitive to their water content. Influenced by the superior hydrophilic properties of cellulose, water molecules absorb on the cellulose surface, swell in the amorphous region, and diffuse between cellulose crystals. Therefore, intermolecular hydrogen bonding between cellulose molecules breaks with the formation of more cellulose-water-cellulose bonds. These internal changes can affect the mechanical properties and change the appearance of the nanocellulose material. For example, Kuang et al. 190 invented a high-performance soft actuator with tremendous promise in soft robotics and biomimetic systems, by controlling the moisture and alignment of cellulose to manage the deformation of nanocellulose. In the moisture absorption process, the swelling of fibers induced by moisture will soften and inflate materials, increasing flexibility and ductility and thus decreasing materials' stiffness and strength. When the water content becomes extremely low, cellulose fibers shrink and crimp to higher stiffness and lower strain. However, the shrinkage and crimping will reduce its evenness and overall strength for materials made up of isotropic (or not strictly aligned) nanocellulose. Thus, an appropriate moisture control might slightly mitigate the stiffness but extend the strain of materials to reach superior strength.

The influence of water on the mechanical properties of the nanocellulose material is complicated. On one hand, it is widely accepted that cellulosic materials have poor water resistance because of the sharply reduced cellulose—cellulose bonds and overall density. The occupation of water between fibers will make fibers slip-like with a plasticizer and finally separate with excess water. Benitez et al. 192 investigated the influence of pH and relative humidity on the tensile strength of isotropic films. They found that an increased humidity dramatically decreased strength and gently extended the strain of materials. After the mixture is soaked in water, the strength and modulus are even worse. However, on the other hand,

water contributes to cellulosic materials' mechanical properties beyond expectation. Petridis et al. ¹⁹³ combined the MD simulation and neutron scattering to investigate the stiffness change of elementary fibrils (36 chains) in different environmental humidities. It has been reported that an appropriate water content will retain the *tg*-conformation of hydroxymethyl of inter chains, enhancing the core stiffness of elementary fibrils. In addition, the formation of bridging hydrogen bonds between interchains O6 and O2 through water molecules will increase the amount of hydrogen bonding, improving the stiffness and strength of the elementary fibrils.

Regarding the macroscale cellulosic material, the slip of the fiber induced by the water absorption must be addressed. It has been reported that the mechanical properties of cotton cloth and flax fiber positively relate to the content of absorbed BW. 194,195 The tensile strength and elongation of cotton cloth increased with a growing moisture content increase while the Young's modulus decreased. 194 Similar results were found in a macroscale fiber constructed with nanocellulose. Mittal et al. 183 reported that the nanocellulose macroscale fiber showed a higher Young's modulus and tensile strength at lower RH. In another example, Hou et al. 196 simulated the interfacial slip between CNC mediated by moisture through MD simulation. They found that the (100) surfaces of CNC with buried -OH groups were bridged to each other through CNC-water-CNC hydrogen bonds, which increased the energy for tensile failure. The CNC films show better tensile strength with no loss in elastic modulus at 20% RH compared with 10% RH. The combination of theoretical simulation and experiments indicated that appropriate water absorption benefits the mechanical properties of cellulosic materials.

In summary, with a water content of lower than around 3%, nanocellulose materials are rigid and will break during elastic deformation (Figure 11). The deformation in this elastic tensile stage is mainly caused by the stretching of nanocellulose without interfacial slipping. On the other hand, with a water content between 3% and 10%, the deformation includes elastic and inelastic stages, which prompts a strong and tough nanocellulose material. In this process, the critical knee point is mainly due to the deformation change from nonslipping to interfacial slipping. During interfacial slipping, the humidity-mediated interface assists in postponing strain localization under single-axial stretching and preventing stress concen-

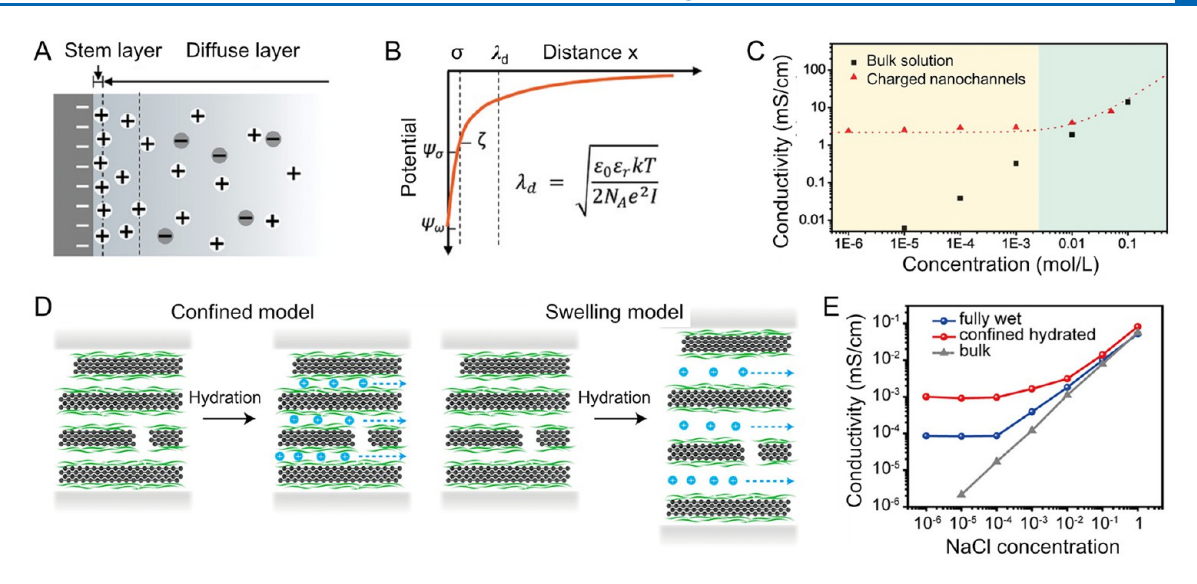


Figure 12. The electrical double-layer theory and its application in cellulose ionic conductors. (A) The electrical double-layer model. (B) The potential on the surface of materials versus the distance. (C) Ion transportation properties of charged nanochannels. (D—E) Schematic description and ion conductivity of nanocellulose channels arranged by graphite under different hydrated levels. (A—C) are reprinted with permission from ref 198. Copyright 2020 John Wiley and Sons. (D, E) are reprinted with permission from ref 201. Copyright 2019 American Chemical Society.

tration. In other words, the humidity-mediated interface can reach a substantially greater fracture strain and resistance than dried nanocellulose due to its higher loading-transfer capabilities. With a water content higher than 10%, the swelling of nanocellulose material reduces the strength. 192,196 When too much water is present at the interfaces, the load transfer is suppressed, and the interfacial strength is reduced. With a water content higher than 25% (the fiber saturation point), the nanocellulose material becomes extremely ductile due to the complete swelling of the nanofibril and penetration of FW.

Influence of Water on the Ionic Properties. Introducing charge groups on nanocellulose has been found to effectively reduce energy consumption during homogenization and convert nanocellulose into an ion-conductive material suitable for various applications. Hydrophilic functional groups, including hydroxyl and carboxyl groups, are electronegative after hydration. Then, these electronegative groups on the cellulose surface attract positive ions by an electrostatic effect. An electrical double-layer model can explain these electrostatic absorption behaviors on the interface between nanocellulose and water (Figure 12A). The first layer of positive ions, closely attracted to the surface of nanocellulose, is called the Stern layer. Under electrostatic force, the concentration of positive ions aggregated near the surface of nanocellulose decreases with increasing distance to the surface and attracts negative ions. This layer, called the diffuse layer, includes attracted ions and their counterions that diffuse from the surface of nanocellulose to its far distance and finally reach a position with zero electrical potential. The distribution of ions in the electrical double-layer model will affect the potential from the surface of nanocellulose to the water.

When the nanocellulose is immersed into an electrolyte, the region of the ion impacted by the electrostatic effect of the surface could be determined by the Debye length. As shown in Figure 12B, the Debye length can be calculated as 198

$$\lambda_{\rm d} = \sqrt{\frac{\varepsilon_0 \varepsilon_{\rm r} kT}{2N_{\rm A} e^2 I}}$$

where I is the ionic strength of the electrolyte, ε_0 is the permittivity of free space, $\varepsilon_{\rm r}$ is the dielectric constant, k is the Boltzmann constant, T is the temperature, $N_{\rm A}$ is Avogadro's number, and e is the elementary charge. When the diameter of the microchannel between nanocellulose is larger than the Debye length, ions will circulate in the microchannel like in bulk water. When the diameter of the nanochannel between nanocelluloses is comparable to or less than the Debye length, ions in the channel will be controlled by the surface electrostatic effect. To summarize, nanofluidic effects regulate the transportation of ions in the nanochannel. The materials show a constant ion conductivity in low-concentration solutions, as shown in Figure 12C.

According to the mechanism of the electrical double layer, Debye length, and nanofluidic effects, the ionic properties of cellulosic materials could be regulated by adjusting the surface charge properties, amounts, and scale of nanochannels. 199,200 For example, the swell of cellulosic materials in water will separate fibrils from each other and thus increase the diameter of the channels in nanocellulose. In a recent study, Zhou et al. 201 constructed a 2D tunable nanochannel for nanofluidic ion transportation through the graphite-cellulose composite. The graphite-cellulose composite shows more than 10 times higher ion conductivity (1 \times 10⁻³ S/cm) than that in the fully swollen state by controlling the hydration degree to confine about a 1 nm nanochannel for ion transportation (Figure 12D,E). Yu et al. 129 prepared fibrous nanofluidic materials with vertically aligned nanochannels constructed by the nanocomposite of nanocellulose and boron nitride nanosheets through 3D printing. The printed aligned BN-CNF ionic cable exhibits a good ionic conductivity of 1.8×10^{-4} S/cm at low salt concentrations ($<10^{-3}$ M). These ionic conductors using cellulosic materials as templates followed by the absorption of an electrolyte solution are also classified as ion reservoirs.²⁰² Water, a commonly used electrolyte solvent, is also used to

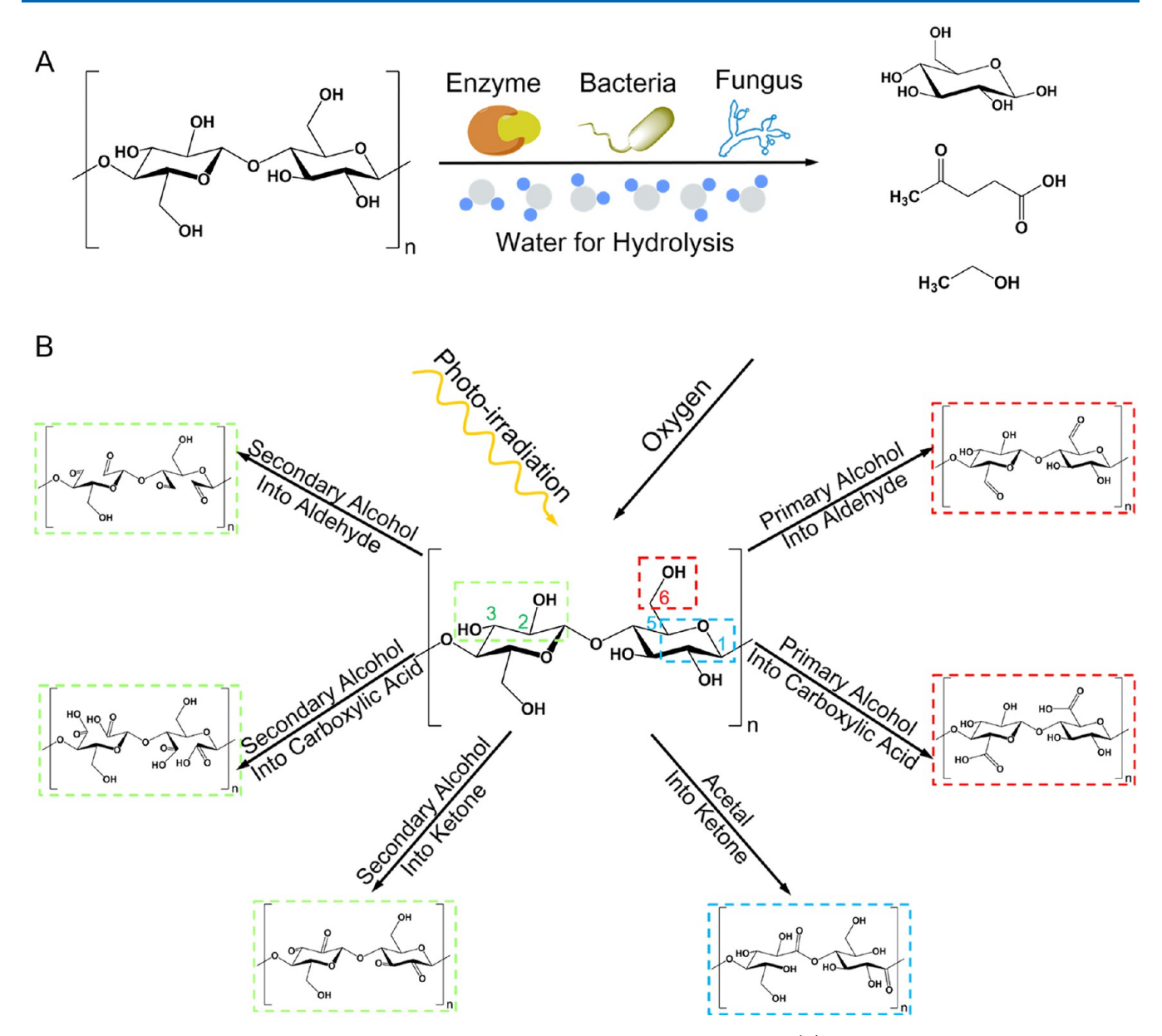


Figure 13. The degradation of cellulose through enzymatic hydrolysis and photo-oxidation. (A) Cellulose degrades through enzymes, bacteria, and fungus catalyzing hydrolysis with sufficient water. (B) Main photo-oxidation reactions of cellulose without water.

construct solvent-containing nanocellulose-based gel ionic conductors. The nanocellulose used to build gel ionic conductors usually needs to be compounded with a polymeric matrix or surface-functionalized to obtain a more stable structure. The selective and rapid transportation on the surface of the cellulose-water interface endows it with extraordinary potential in applications such as batteries and fuel cells. Huang et al. built an ultrathin CNF ion redistributor and applied it in aqueous zinc batteries. The CNF thin films exhibit a negligibly negative effect on the ionic conductivity of electrolytes and excellent performance in addressing the dendrite formation, showing a promising and sustainable route toward dendrite-free Zn anode for aqueous zinc batteries.

In addition to nanocellulose materials applied as ionic conductors, cellulosic materials have long been used in electrical insulators, oil-filled power transformers, and paper-insulated power cables due to their excellent breakdown

strength and resistivity. 204 The dielectric properties of materials are significantly affected by the frequency, temperature, moisture, and density. Oil impregnation is commonly used to reduce moisture adsorption and remove air to enhance the dielectric properties of the insulation paper. Besides, nanocellulose, as a nanofiller, can significantly improve the paper density and insulation properties. The relative dielectric constant (ε_r) of nanocellulose paper with a dense nanostructure reaches 5.3 (at 1.1 GHz), a value significantly higher than the relative dielectric constant (1.3-4.0) typically found in porous traditional paper. 205-207 Huang et al. 208 introduced nanocellulose as a nanofiller in softwood fiber to decrease pore size and air voids and thereby dramatically improve the dielectric breakdown behavior of insulating paper. In AC breakdown results, the scale parameter increases from 10.6 to 13.5 kV/mm for nanocellulose-modified paper, while for DC breakdown fields, the addition of nanocellulose to softwood

fiber results in the highest breakdown strength, showing an enhancement of about 21%.

Influence of Water on the Degradability. Cellulose is a stable and strong material, yet its moisture sensitivity and nature as a polysaccharide make it degradable to some fungi and bacteria in the air, water, and soil.²⁰⁹ In an aqueous solution, cellulose could be hydrolyzed into glucose, levulinic acid, and ethanol by microbial fermentation (Figure 13A). In this process, water, as an indispensable part of the biological system, mediates many biochemical reactions by acting as a solvent and reactant. Water also plays a vital role in adhesion medium, cell morphology, and other cellular functions.²¹⁰ Therefore, water on the surface of cellulose nanofibers creates a biofilm with heat and dirt in the air during the growth of fungi and bacteria and causes biodegradation. After that, fungi attack fibers from inside toward the outer layer of fibers, while bacteria start attacking from the fiber surface toward the inner part.²¹¹ Therefore, the widely accepted approach to prevent the growth of microorganisms and restrain enzymatic hydrolysis is the application of water- and oil-repellent finishes. These finishes can cause a significant drop in fiber wettability. 209,212-214 In addition, since the amorphous region is more accessible to water than the crystalline region in cellulose, the biodegradation of cellulose is also highly related to its crystallinity. For example, Park et al.²¹³ analyzed the correlation of factors influencing the biodegradability of cellulose fabric. They found that moisture regain was the most influential factor, and the crystallinity negatively correlated with enzyme hydrolysis.

Additionally, based on the understanding of the hydrophilicity of cellulose—the interaction between water and hydroxyl groups on the surface of cellulose—reducing the exposure of hydroxyl groups through chemical treatment such as a cross-linkage technique has been proved to have more potential to hinder the biodegradation process of cellulosic material. Moreover, cellulose is a preeminent feedstuff for microbial fuel cells as a sustainable and biodegradable polysaccharide with no food conflicts. Microbiological degradation of cellulose depends on the enzyme catalyzing breaking of the β -1,4 glycosidic bond with glucose production, as the energy supply of microorganisms can transfer electrons to anodes by digesting the substrates.

Although nanocellulose materials are sensitive to moisture, the controllable preparation of high-density nanocellulose materials can achieve better water penetration resistance and antibacterial functions while significantly reducing pores and exposed hydroxyl groups. Moreover, after compounding with other packaging materials, nanocellulose, as a nanofiller, can improve the mechanical properties, water vapor barrier, and antibacterial properties of the materials.²²⁰ In addition, nanocellulose can also degrade when the water content is low, further improving the degradability of the material. Without water, nanocellulose can be slowly degraded by photodegradation and photo-oxidation. Under the irradiation of light, especially UV light, cellulose can be photo-oxidized and degraded by the initiators that absorb energy during irradiation.²²¹ Some reports suggested that carbon-centered radicals were generated during photo-oxidation. Oxygen is then added to form peroxyl radicals, and the abstracted hydrogen will subsequently form hydroperoxides. 221,222 After the energy from UV light is absorbed, hydroperoxides decompose into extremely reactive hydroxyl radicals, which can oxidize cellulose by photodegradation. The oxidation of cellulose has been widely studied, and possible oxidation reaction sites and products are summarized and listed in Figure 13B. Because of their extreme reactivity, hydroxyl radicals react with carbohydrates and abstract hydrogen atoms bound to carbon in an essentially statistical way without showing any preference. ^{221,223}.

In summary, the fact that moisture absorption promotes chemical and microbial hydrolysis of nanocellulose indicates the degradability of nanocellulose and its limited material stability and validity with water. However, the nanocellulose material can achieve greater stability and an extended product lifetime by enhancing water resistance, albeit at the cost of reduced biodegradability. Li et al.² thoroughly discussed and proposed strategies for striking a balance between enhanced product stability and improved biodegradability. Techniques such as ion cross-linking, intercalation, and reversible chemical reactions and surface superhydrophobization treatment were considered promising approaches to enhance the durability of cellulosic materials without sacrificing their biodegradability.²

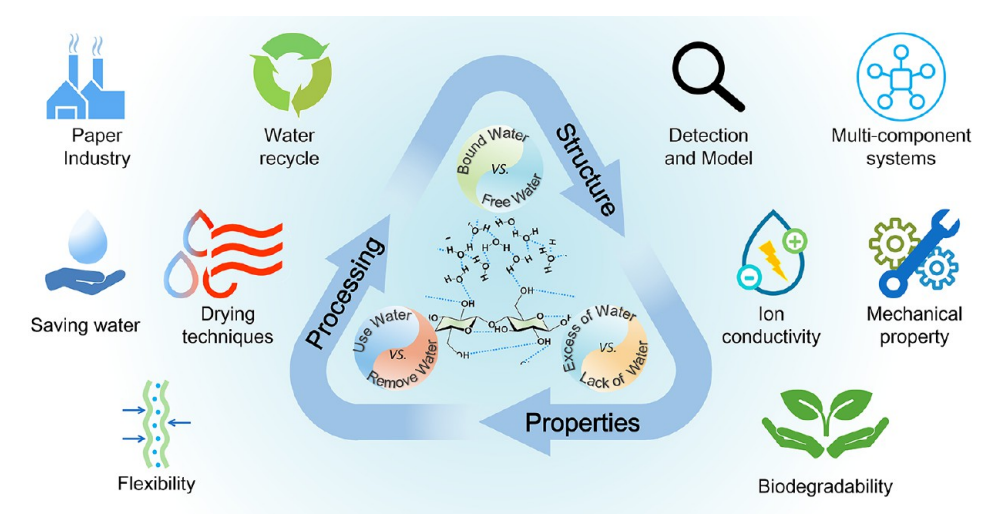
CONCLUSIONS AND PERSPECTIVES

Nanocellulose has garnered extensive attention and has been applied in biomedical applications, energy storage, water treatment, 3D printing, optical devices, textiles, and food packing. However, its inherent sensitivity to moisture poses challenges in terms of storage, transportation, and drying. An in-depth understanding of the interplay between nanocellulose and water holds the potential to not only reduce production costs but also revolutionize the design of nanocellulose-based functional materials.

By categorizing water into BW and FW based on its interaction with nanocellulose, we can better understand the critical role of water in influencing material properties. Representative methods, including IR, Raman spectroscopy, NMR, DSC, and DTA, can be used to analyze the distribution of BW and FW and the water-nanocellulose interaction. However, there is still some debate regarding water distribution when these methods are combined with computational techniques. While visual monitoring vividly illustrates the distribution and movement of water within materials, current technologies are limited in resolution, typically at the micrometer level, which lacks precision. Future trends in this field are expected to involve in-depth analysis and identification of water-cellulose interactions through monitoring and computational modeling techniques like molecular dynamics (MD), providing a more comprehensive understanding of water-nanocellulose interactions. 224

A deeper understanding of the crucial role that water plays in regulating the - bonding network, dielectric properties, and accessibility of active sites on nanocellulose can assist us in purposefully tuning material properties, such as mechanical characteristics, ionic conductivity, and biodegradability. However, current research still faces challenges in accurately controlling the water distribution and achieving a profound comprehension of water—nanocellulose interactions. Besides, water could also be applied to manipulate cellulose dynamics in multicomponent systems, including lignocellulose/DES/water, ²²⁵ cellulose/IL/water, ²²⁶ and cellulose/polyacrylamide/water, ²²⁷ and modulate the material ionic conductivity, adhesion, and mechanical properties. Further research into complex multicomponent systems is essential to expand our understanding of the critical role of water in cellulosic materials.

Scheme 1. Critical Role of Water in (1) Dispersing, Transforming, and Assembling Nanocellulose, (2) Softening, Tangling, and Bridging Nanofibers, and (3) Regulating the Hydrogen Bonding Network, Dielectric Properties, and Accessibility of Active Sites within Nanocellulose⁴



^aAn in-depth understanding offers benefits in investigating nanocellulose multicomponent systems, fine-tuning materials properties, conserving water and energy resources, and ultimately enhancing environmental sustainability.

Water serves various vital roles in assembling and modifying cellulosic materials, acting as a suspending and reaction medium and a hydrogen bond bridge. Wet nanofibers maintain the morphological structure of nanocellulose but come with increased transportation costs and the risk of spoilage. Dry nanocellulose, on the other hand, is affected by issues such as fiber entanglement and hornification, making it challenging to obtain dispersions that match the morphological structure of raw materials. Current research predominantly focuses on surface charge modification, steric hindrance enhancement, solvent exchange, and controlled drying processes, yet further investigations are required to find more economical and practical solutions. 1777

Water plays multiple roles in the cellulose industry, including acting as a suspending medium and swelling agent for fibers, a solvent for chemicals and additives, a dispersant and transport medium for fibers, and an aid in materialforming processes. Despite the maturity of the modern cellulose industry, water resource recovery has always been a significant challenge faced by this sector. Currently, water cycling in the industrial sector primarily focuses on processing process water and wastewater, 228 lacking innovation in implementing water-saving techniques during production. In the context of sustainable development, a profound understanding of the interactions between water and cellulose and the subsequent application of this understanding in waterefficient production, energy efficiency improvement, and carbon emission reduction are of paramount importance. This comprehension not only helps reduce the waste of water resources but also promotes more sustainable production methods in the industry, aligning with environmental conservation and energy-saving requirements.

Furthermore, water-driven cellulosic material construction and industrial development exhibit significant characteristics during production, including sustainability, environmental friendliness, low cost, and ease of scalability. By gaining an in-depth understanding of the role of water in nanocellulose material structures, properties, and processing, as shown in Scheme 1, we can improve water's efficient utilization and

circulation, reduce water consumption, lower material drying and shaping costs, and further enhance the environmental sustainability of the production and materials.

AUTHOR INFORMATION

Corresponding Authors

Chaoji Chen — Department of Materials Science and
Engineering, University of Maryland, College Park, Maryland
20742, United States; Email: chenchaojili@whu.edu.cn

Teng Li — Department of Mechanical Engineering, University
of Maryland, College Park, Maryland 20742, United States;
orcid.org/0000-0001-6252-561X; Email: lit@umd.edu

Liangbing Hu — Department of Materials Science and
Engineering, University of Maryland, College Park, Maryland
20742, United States; Center for Materials Innovation,
University of Maryland, College Park, Maryland 20742,
United States; orcid.org/0000-0002-9456-9315;
Email: binghu@umd.edu

Authors

Shuangshuang Jing — Department of Materials Science and Engineering, University of Maryland, College Park, Maryland 20742, United States

Lianping Wu — Department of Mechanical Engineering, University of Maryland, College Park, Maryland 20742, United States; orcid.org/0000-0002-6865-6386

Amanda P. Siciliano – Department of Materials Science and Engineering, University of Maryland, College Park, Maryland 20742, United States

Complete contact information is available at: https://pubs.acs.org/10.1021/acsnano.3c06773

Notes

The authors declare no competing financial interest.

ACKNOWLEDGMENTS

We acknowledge the support of the A. James Clark School, University of Maryland, and the support of the National Science Foundation, USA (Grants CMMI # 1936452).

VOCABULARY

bound water water molecules firmly bound on the surface of fibers

free water water molecules surrounding fibers with mobility and thermal

properties closely resembling those of bulk water

hygroscopicity water absorption capacity of

nanocellulose materials, significantly influenced by factors such as the specific surface area, dimensions, and surface func-

tional groups

rehydration and reformation the absorption of water by

nanocellulose materials, resulting in improved elasticity and moldability, primarily due to the

plasticizing effect of water

ambient drying the process of drying nano-

cellulose materials in the surrounding environment with minimal energy input, which can be enhanced through techniques such as solvent exchange, ion cross-linking, freeze cross-

linking, etc.

ion conductivity the ability of nanocellulose

materials to transport ions modulated by water, which plays a role in constructing and controlling the size of nanochannels within nanocellulose

ion conductors

REFERENCES

- (1) Eichhorn, S. J.; Dufresne, A.; Aranguren, M.; Marcovich, N.; Capadona, J.; Rowan, S. J.; Weder, C.; Thielemans, W.; Roman, M.; Renneckar, S.; et al. Current International Research into Cellulose Nanofibres and Nanocomposites. *J. Mater. Sci.* **2010**, *45*, 1–33.
- (2) Li, T.; Chen, C.; Brozena, A. H.; Zhu, J.; Xu, L.; Driemeier, C.; Dai, J.; Rojas, O. J.; Isogai, A.; Wågberg, L.; et al. Developing Fibrillated Cellulose as a Sustainable Technological Material. *Nature* **2021**, *590*, 47–56.
- (3) Man, Y.; Han, Y.; Wang, Y.; Li, J.; Chen, L.; Qian, Y.; Hong, M. Woods to Goods: Water Consumption Analysis for Papermaking Industry in China. *J. Cleaner Prod.* **2018**, *195*, 1377–1388.
- (4) Suhr, M.; Klein, G.; Kourti, I.; Rodrigo Gonzalo, M.; Giner Santonja, G.; Roudier, S.; Delgado Sancho, L. Best Available Techniques (BAT) Reference Document for the Production of Pulp, Paper and Board. *Industrial Emissions Directive* 2010/75/EU (Integrated Pollution Prevention and Control). EUR 27235. Luxembourg (Luxembourg): Publications Office of the European Union; 2015, JRC95678.
- (5) Xiao, S.; Chen, C.; Xia, Q.; Liu, Y.; Yao, Y.; Chen, Q.; Hartsfield, M.; Brozena, A.; Tu, K.; Eichhorn, S.; et al. Lightweight, Strong, Moldable Wood via Cell Wall Engineering as a Sustainable Structural Material. *Science* **2021**, *374*, 465–471.

- (6) Vilarinho, F.; Sanches Silva, A.; Vaz, M. F.; Farinha, J. P. Nanocellulose in Green Food Packaging. *Crit. Rev. Food Sci. Nutr.* **2018**, *58*, 1526–1537.
- (7) de Amorim, J. D. P.; de Souza, K. C.; Duarte, C. R.; da Silva Duarte, I.; Ribeiro, F. d. A. S.; Silva, G. S.; de Farias, P. M. A.; Stingl, A.; Costa, A. F. S.; Vinhas, G. M.; et al. Plant and Bacterial Nanocellulose: Production, Properties and Applications in Medicine, Food, Cosmetics, Electronics and Engineering. a Review. *Environ. Chem. Lett.* **2020**, *18*, 851–869.
- (8) Fang, Z.; Zhu, H.; Yuan, Y.; Ha, D.; Zhu, S.; Preston, C.; Chen, Q.; Li, Y.; Han, X.; Lee, S.; et al. Novel Nanostructured Paper with Ultrahigh Transparency and Ultrahigh Haze for Solar Cells. *Nano Lett.* **2014**, *14*, 765–773.
- (9) Du, X.; Zhang, Z.; Liu, W.; Deng, Y. Nanocellulose-Based Conductive Materials and Their Emerging Applications in Energy Devices-a Review. *Nano Energy* **2017**, *35*, 299–320.
- (10) Mahfoudhi, N.; Boufi, S. Nanocellulose as a Novel Nanostructured Adsorbent for Environmental Remediation: a Review. *Cellulose* **2017**, *24*, 1171–1197.
- (11) Eichhorn, S. J.; Etale, A.; Wang, J.; Berglund, L. A.; Li, Y.; Cai, Y.; Chen, C.; Cranston, E. D.; Johns, M. A.; Fang, Z. Current International Research into Cellulose as a Functional Nanomaterial for Advanced Applications. *J. Mater. Sci.* **2022**, *57*, 5697–5767.
- (12) Rahman, M.; Avelin, A.; Kyprianidis, K. a Review on the Modeling, Control and Diagnostics of Continuous Pulp Digesters. *Processes* **2020**, *8*, 1231.
- (13) Heiner, A. P.; Kuutti, L.; Teleman, O. Comparison of the Interface Between Water and Four Surfaces of Native Crystalline Cellulose by Molecular Dynamics Simulations. *Carbohydr. Res.* **1998**, 306, 205–220.
- (14) Kerch, G. Distribution of Tightly and Loosely Bound Water in Biological Macromolecules and Age-Related Diseases. *Int. J. Biol. Macromol.* **2018**, *118*, 1310–1318.
- (15) Benselfelt, T.; Kummer, N.; Nordenström, M.; Fall, A. B.; Nyström, G.; Wågberg, L. the Colloidal Properties of Nanocellulose. *ChemSusChem* **2023**, *16*, No. e202201955.
- (16) Olsson, A.-M.; Salmén, L. the Association of Water to Cellulose and Hemicellulose in Paper Examined by Ftir Spectroscopy. *Carbohydr. Res.* **2004**, 339, 813–818.
- (17) Paladini, G.; Venuti, V.; Crupi, V.; Majolino, D.; Fiorati, A.; Punta, C. FTIR-ATR Analysis of the H-Bond Network of Water in Branched Polyethyleneimine/Tempo-Oxidized Cellulose Nano-Fiber Xerogels. *Cellulose* **2020**, 27, 8605–8618.
- (18) Velazquez, G.; Herrera-Gómez, A.; Martín-Polo, M. Identification of Bound Water through Infrared Spectroscopy in Methylcellulose. *J. Food Eng.* **2003**, *59*, 79–84.
- (19) Watanabe, A.; Morita, S.; Kokot, S.; Matsubara, M.; Fukai, K.; Ozaki, Y. Drying Process of Microcrystalline Cellulose Studied by Attenuated Total Reflection IR Spectroscopy with Two-Dimensional Correlation Spectroscopy and Principal Component Analysis. *J. Mol. Struct.* **2006**, 799, 102–110.
- (20) Watanabe, A.; Morita, S.; Ozaki, Y. a Study on Water Adsorption Onto Microcrystalline Cellulose by Near-Infrared Spectroscopy with Two-Dimensional Correlation Spectroscopy and Principal Component Analysis. *Appl. Spectrosc.* **2006**, *60*, 1054–1061. (21) Sekine, Y.; Ikeda-Fukazawa, T. Structural Changes of Water in a
- (21) Sekine, Y.; Ikeda-Fukazawa, T. Structural Changes of Water in Hydrogel During Dehydration. *J. Chem. Phys.* **2009**, *130*, 034501.
- (22) Kudo, K.; Ishida, J.; Syuu, G.; Sekine, Y.; Ikeda-Fukazawa, T. Structural Changes of Water in Poly (Vinyl Alcohol) Hydrogel During Dehydration. *J. Chem. Phys.* **2014**, *140*, 044909.
- (23) O'Neill, H.; Pingali, S. V.; Petridis, L.; He, J.; Mamontov, E.; Hong, L.; Urban, V.; Evans, B.; Langan, P.; Smith, J. C.; et al. Dynamics of Water Bound to Crystalline Cellulose. *Sci. Rep.* **2017**, *7*, 1–13.
- (24) Zhao, H.; Chen, Z.; Du, X.; Chen, L. Contribution of Different State of Adsorbed Water to the Sub-Tg Dynamics of Cellulose. *Carbohydr. Polym.* **2019**, 210, 322–331.

- (25) Felby, C.; Thygesen, L. G.; Kristensen, J. B.; Jørgensen, H.; Elder, T. Cellulose—Water Interactions During Enzymatic Hydrolysis as Studied by Time Domain NMR. *Cellulose* **2008**, *15*, 703—710.
- (26) Hatakeyama, T.; Nakamura, K.; Hatakeyama, H. Determination of Bound Water Content in Polymers by DTA, DSC and TG. *Thermochim. Acta* 1988, 123, 153–161.
- (27) Bedane, A. H.; Xiao, H.; Eić, M.; Farmahini-Farahani, M. Structural and Thermodynamic Characterization of Modified Cellulose Fiber-Based Materials and Related Interactions with Water Vapor. *Appl. Surf. Sci.* **2015**, *351*, 725–737.
- (28) Park, S.; Venditti, R. A.; Jameel, H.; Pawlak, J. J. Hard to Remove Water in Cellulose Fibers Characterized by High Resolution Thermogravimetric Analysis-Methods Development. *Cellulose* **2006**, 13, 23–30.
- (29) Amini, E. N.; Tajvidi, M.; Bousfield, D. W.; Gardner, D. J.; Shaler, S. M. Dewatering Behavior of a Wood-Cellulose Nanofibril Particulate System. *Sci. Rep.* **2019**, *9*, 1–10.
- (30) Ma, T.; Morita, G.; Inagaki, T.; Tsuchikawa, S. Moisture Transport Dynamics in Wood During Drying Studied by Long-Wave Near-Infrared Hyperspectral Imaging. *Cellulose* **2022**, *29*, 133–145.
- (31) Li, D.; Zhu, Z.; Sun, D.-W. Visualization and Quantification of Content and Hydrogen Bonding State of Water in Apple and Potato Cells by Confocal Raman Microscopy: a Comparison Study. *Food Chem.* **2022**, 385, 132679.
- (32) Li, D.; Zhu, Z.; Sun, D.-W. Visualization of the in situ Distribution of Contents and Hydrogen Bonding States of Cellular Level Water in Apple Tissues by Confocal Raman Microscopy. *Analyst* **2020**, *145*, 897–907.
- (33) Ponzecchi, A.; Thybring, E. E.; Digaitis, R.; Fredriksson, M.; Solsona, S. P.; Thygesen, L. G. Raman Micro-Spectroscopy of Two Types of Acetylated Norway Spruce Wood at Controlled Relative Humidity. *Front. Plant Sci.* **2022**, *13*, 986578.
- (34) Sedighi-Gilani, M.; Griffa, M.; Mannes, D.; Lehmann, E.; Carmeliet, J.; Derome, D. Visualization and Quantification of Liquid Water Transport in Softwood by Means of Neutron Radiography. *Int. J. Heat Mass Transfer* **2012**, *55*, 6211–6221.
- (35) Bridarolli, A.; Odlyha, M.; Burca, G.; Duncan, J. C.; Akeroyd, F. A.; Church, A.; Bozec, L. Controlled Environment Neutron Radiography of Moisture Sorption/Desorption in Nanocellulose-Treated Cotton Painting Canvases. *ACS Appl. Polym. Mater.* **2021**, 3, 777–788.
- (36) Das, R.; Deshpande, V. S.; Fleck, N. A. the Transport of Water in a Cellulose Foam. *EML* **2022**, *57*, 101897.
- (37) Geng, S.; Wang, H.; Wang, X.; Ma, X.; Xiao, S.; Wang, J.; Tan, M. a Non-Invasive NMR and MRI Method to Analyze the Rehydration of Dried Sea Cucumber. *Anal. Methods* **2015**, *7*, 2413–2419.
- (38) Leisen, J.; Hojjatie, B.; Coffin, D. W.; Lavrykov, S. A.; Ramarao, B. V.; Beckham, H. W. Through-Plane Diffusion of Moisture in Paper Detected by Magnetic Resonance Imaging. *Ind. Eng. Chem. Res.* **2002**, *41*, 6555–6565.
- (39) Ben Abdelouahab, N.; Gossard, A.; Ma, X.; Dialla, H.; Maillet, B.; Rodts, S.; Coussot, P. Understanding Mechanisms of Drying of a Cellulose Slurry by Magnetic Resonance Imaging. *Cellulose* **2021**, *28*, 5321–5334.
- (40) Zhang, C.; He, Y.; Zheng, Y.; Ai, C.; Cao, H.; Xiao, J.; El-Seedi, H.; Chen, L.; Teng, H. Effect of Carboxymethyl Cellulose (CMC) on Some Physico-Chemical and Mechanical Properties of Unrinsed Surimi Gels. *LWT* **2023**, *180*, 114653.
- (41) He, Y.; Chen, Q.; Yang, L.; Liu, X.; Hu, J.; Jiang, T. Study on the Diffusion Behavior of Moisture in New and Aged Oil-Paper Insulation by Terahertz Imaging Technology. In 2023 IEEE 4th International Conference on Electrical Materials and Power Equipment (ICEMPE), 2023/05/07; IEEE: 2023; pp 1–4. DOI: 10.1109/ICEMPE57831.2023.10139356.
- (42) Varga, B.; Migliardo, F.; Takacs, E.; Vertessy, B.; Magazù, S.; Telling, M. Study of Solvent-Protein Coupling Effects by Neutron Scattering. *J. Biol. Phys.* **2010**, *36*, 207–220.

- (43) Fredriksson, M.; Thygesen, L. G. the States of Water in Norway Spruce (Picea Abies (L.) Karst.) Studied By Low-Field Nuclear Magnetic Resonance (LF-NMR) Relaxometry: Assignment of Free-Water Populations Based on Quantitative Wood Anatomy. *Holzforschung* **2017**, *71*, *77*–90.
- (44) Araujo, C. D. Proton Magnetic Resonance of Wood And Water in Wood; University of British Columbia: 1993.
- (45) Bag, M. A.; Valenzuela, L. M. Impact of the Hydration States of Polymers on Their Hemocompatibility for Medical Applications: a Review. *Int. J. Mol. Sci.* **2017**, *18*, 1422.
- (46) Miwa, Y.; Ishida, H.; Tanaka, M.; Mochizuki, A. 2H-NMR and 13C-NMR Study of the Hydration Behavior of Poly (2-Methoxyethyl Acrylate), Poly (2-Hydroxyethyl Methacrylate) and Poly (Tetrahydrofurfuryl Acrylate) in Relation to Their Blood Compatibility As Biomaterials. *J. Biomater. Sci., Polym. Ed.* **2010**, *21*, 1911–1924.
- (47) Froix, M. F.; Nelson, R. the Interaction of Water with Cellulose From Nuclear Magnetic Resonance Relaxation Times. *Macromolecules* **1975**, *8*, 726–730.
- (48) Nakaoki, T.; Yamashita, H. Bound States of Water in Poly (Vinyl Alcohol) Hydrogel Prepared by Repeated Freezing and Melting Method. *J. Mol. Struct.* **2008**, 875, 282–287.
- (49) Hatakeyama, H.; Hatakeyama, T. Interaction between Water and Hydrophilic Polymers. *Thermochim. Acta* **1998**, *308*, 3–22.
- (50) Zhou, X.; Zhao, F.; Guo, Y.; Rosenberger, B.; Yu, G. Architecting Highly Hydratable Polymer Networks to Tune the Water State for Solar Water Purification. *Sci. Adv.* **2019**, *S*, No. eaaw5484.
- (51) Li, D.; Zhu, Z.; Sun, D.-W. Quantification of Hydrogen Bonding Strength of Water in Saccharide Aqueous Solutions by Confocal Raman Microscopy. *J. Mol. Liq.* **2021**, *342*, 117498.
- (52) Blümler, P.; Blümich, B.; Botto, R. E.; Fukushima, E. Spatially Resolved Magnetic Resonance: Methods, Materials, Medicine, Biology, Rheology, Geology, Ecology, Hardware; Wiley: 2008.
- (53) Dvinskikh, S. V.; Henriksson, M.; Mendicino, A. L.; Fortino, S.; Toratti, T. NMR Imaging Study and Multi-Fickian Numerical Simulation of Moisture Transfer in Norway Spruce Samples. *Eng. Struct.* **2011**, *33*, 3079–3086.
- (54) Hameury, S.; Sterley, M. Magnetic Resonance Imaging of Moisture Distribution in Pinus Sylvestris L. Exposed to Daily Indoor Relative Humidity Fluctuations. *Wood Mater. Sci. Eng.* **2006**, *1*, 116–126.
- (55) Zhao, F.; Guo, Y.; Zhou, X.; Shi, W.; Yu, G. Materials for Solar-Powered Water Evaporation. *Nat. Rev. Mater.* **2020**, *5*, 388–401.
- (56) Guan, Q.-F.; Han, Z.-M.; Ling, Z.-C.; Yang, H.-B.; Yu, S.-H. Sustainable Wood-Based Hierarchical Solar Steam Generator: a Biomimetic Design with Reduced Vaporization Enthalpy of Water. *Nano Lett.* **2020**, *20*, 5699–5704.
- (57) Paajanen, A.; Ceccherini, S.; Maloney, T.; Ketoja, J. A. Chirality and Bound Water in the Hierarchical Cellulose Structure. *Cellulose* **2019**, *26*, 5877–5892.
- (58) Guo, X.; Wu, Y.; Xie, X. Water Vapor Sorption Properties of Cellulose Nanocrystals and Nanofibers Using Dynamic Vapor Sorption Apparatus. *Sci. Rep.* **2017**, *7*, 1–12.
- (59) Mihranyan, A.; Llagostera, A. P.; Karmhag, R.; Strømme, M.; Ek, R. Moisture Sorption by Cellulose Powders of Varying Crystallinity. *Int. J. Pharm.* **2004**, 269, 433–442.
- (60) Driemeier, C.; Mendes, F. M.; Oliveira, M. M. Dynamic Vapor Sorption and Thermoporometry to Probe Water in Celluloses. *Cellulose* **2012**, *19*, 1051–1063.
- (61) Lowell, S.; Shields, J. E.; Thomas, M. A.; Thommes, M. Characterization of Porous Solids and Powders: Surface Area, Pore Size And Density; Springer Science & Business Media: 2006.
- (62) Hakalahti, M.; Faustini, M.; Boissière, C.; Kontturi, E.; Tammelin, T. Interfacial Mechanisms of Water Vapor Sorption into Cellulose Nanofibril Films as Revealed by Quantitative Models. *Biomacromolecules* **2017**, *18*, 2951–2958.
- (63) Hatakeyama, T.; Inui, Y.; Iijima, M.; Hatakeyama, H. Bound Water Restrained by Nanocellulose Fibres. *J. Therm. Anal. Calorim.* **2013**, *113*, 1019–1025.

- (64) Ul-Islam, M.; Khan, T.; Park, J. K. Water Holding and Release Properties of Bacterial Cellulose Obtained by in situ and ex situ Modification. *Carbohydr. Polym.* **2012**, *88*, 596–603.
- (65) Ul-Islam, M.; Shah, N.; Ha, J. H.; Park, J. K. Effect of Chitosan Penetration on Physico-Chemical and Mechanical Properties of Bacterial Cellulose. *Korean J. Chem. Eng.* **2011**, 28, 1736–1743.
- (66) Li, Y.; Liu, Y.; Liu, Y.; Lai, W.; Huang, F.; Ou, A.; Qin, R.; Liu, X.; Wang, X. Ester Crosslinking Enhanced Hydrophilic Cellulose Nanofibrils Aerogel. ACS Sustainable Chem. Eng. 2018, 6, 11979—11988.
- (67) Jiang, F.; Hsieh, Y.-L. Amphiphilic Superabsorbent Cellulose Nanofibril Aerogels. *J. Mater. Chem. A* **2014**, *2*, 6337–6342.
- (68) Fang, L.; Catchmark, J. M. Structure Characterization of Native Cellulose During Dehydration and Rehydration. *Cellulose* **2014**, *21*, 3951–3963.
- (69) Tolonen, L. K.; Bergenstråhle-Wohlert, M.; Sixta, H.; Wohlert, J. Solubility of Cellulose in Supercritical Water Studied by Molecular Dynamics Simulations. *J. Phys. Chem. B* **2015**, *119*, 4739–4748.
- (70) Adschiri, T.; Hirose, S.; Malaluan, R.; Arai, K. Noncatalytic Conversion of Cellulose in Supercritical and Subcritical Water. *J. Chem. Eng. Jpn.* **1993**, *26*, 676–680.
- (71) Lindman, B.; Karlström, G.; Stigsson, L. on the Mechanism of Dissolution of Cellulose. *J. Mol. Liq.* **2010**, *156*, 76–81.
- (72) Bergensträhle, M.; Wohlert, J.; Himmel, M. E.; Brady, J. W. Simulation Studies of The Insolubility of Cellulose. *Carbohydr. Res.* **2010**, 345, 2060–2066.
- (73) Medronho, B.; Romano, A.; Miguel, M. G.; Stigsson, L.; Lindman, B. Rationalizing Cellulose (in) Solubility: Reviewing Basic Physicochemical Aspects and Role of Hydrophobic Interactions. *Cellulose* **2012**, *19*, 581–587.
- (74) Gross, A. S.; Chu, J.-W. on the Molecular Origins of Biomass Recalcitrance: the Interaction Network and Solvation Structures of Cellulose Microfibrils. *J. Phys. Chem. B* **2010**, *114*, 13333–13341.
- (75) Miyamoto, H.; Schnupf, U.; Brady, J. W. Water Structuring over the Hydrophobic Surface of Cellulose. *J. Agric. Food Chem.* **2014**, 62, 11017–11023.
- (76) Bao, Y.; Qian, H.-j.; Lu, Z.-y.; Cui, S. Revealing the Hydrophobicity of Natural Cellulose by Single-Molecule Experiments. *Macromolecules* **2015**, *48*, 3685–3690.
- (77) Cosgrove, D. J. Re-Constructing Our Models of Cellulose and Primary Cell Wall Assembly. *Curr. Opin. Plant Biol.* **2014**, 22, 122–131.
- (78) Fernandes, A. N.; Thomas, L. H.; Altaner, C. M.; Callow, P.; Forsyth, V. T.; Apperley, D. C.; Kennedy, C. J.; Jarvis, M. C. Nanostructure of Cellulose Microfibrils in Spruce Wood. *Proc. Natl. Acad. Sci.* 2011, 108, E1195–E1203.
- (79) Sobue, H.; Kiessig, H.; Hess, K. Das System Cellulose–Natriumhydroxyd–Wasser in Abhängigkeit von der Temperatur. Zeitschrift für Physikalische Chemie 1939, 43B, 309–328.
- (80) Yamashiki, T.; Kamide, K.; Okajima, K.; Kowsaka, K.; Matsui, T.; Fukase, H. Some Characteristic Features of Dilute Aqueous Alkali Solutions of Specific Alkali Concentration (2.5 mol L⁻¹) Which Possess Maximum Solubility Power Against Cellulose. *Polym. J.* **1988**, 20, 447–457.
- (81) Xiong, B.; Zhao, P.; Cai, P.; Zhang, L.; Hu, K.; Cheng, G. NMR Spectroscopic Studies on the Mechanism of Cellulose Dissolution in Alkali Solutions. *Cellulose* **2013**, *20*, 613–621.
- (82) Dong, Q.; Zhang, X.; Qian, J.; He, S.; Mao, Y.; Brozena, A. H.; Zhang, Y.; Pollard, T. P.; Borodin, O. A.; Wang, Y.; et al. a Cellulose-Derived Supramolecule for Fast Ion Transport. *Sci. Adv.* **2022**, *8*, No. eadd2031.
- (83) Qian, J.; Dong, Q.; Chun, K.; Zhu, D.; Zhang, X.; Mao, Y.; Culver, J. N.; Tai, S.; German, J. R.; Dean, D. P.; et al. Highly Stable, Antiviral, Antibacterial Cotton Textiles via Molecular Engineering. *Nat. Nanotechnol.* **2023**, *18*, 1–9.
- (84) Liebert, T. Cellulose Solvents-Remarkable History, Bright Future. In *Cellulose solvents: for analysis, shaping and chemical modification*; ACS Publications: 2010; pp 3–54.

- (85) Saalwächter, K.; Burchard, W.; Klüfers, P.; Kettenbach, G.; Mayer, P.; Klemm, D.; Dugarmaa, S. Cellulose Solutions in Water Containing Metal Complexes. *Macromolecules* **2000**, 33, 4094–4107.
- (86) Alexandridis, P.; Ghasemi, M.; Furlani, E. P.; Tsianou, M. Solvent Processing of Cellulose for Effective Bioresource Utilization. *Curr. Opin. Green Sustainable Chem.* **2018**, *14*, 40–52.
- (87) Cai, J.; Zhang, L. Rapid Dissolution of Cellulose in Lioh/Urea and Naoh/Urea Aqueous Solutions. *Macromol. Biosci.* **2005**, *5*, 539–548.
- (88) Zhang, L.; Ruan, D.; Gao, S. Dissolution and Regeneration of Cellulose in NaOH/Thiourea Aqueous Solution. *J. Polym. Sci., Part B: Polym. Phys.* **2002**, *40*, 1521–1529.
- (89) Yan, L.; Gao, Z. Dissolving of Cellulose in PEG/NaOH Aqueous Solution. *Cellulose* **2008**, *15*, 789–796.
- (90) Yamane, C.; Miyamoto, H.; Hayakawa, D.; Ueda, K. Folded-Chain Structure of Cellulose II Suggested by Molecular Dynamics Simulation. *Carbohydr. Res.* **2013**, *379*, 30–37.
- (91) Adusumali, R. B.; Reifferscheid, M.; Weber, H.; Roeder, T.; Sixta, H.; Gindl, W. Mechanical Properties of Regenerated Cellulose Fibres for Composites. *Macromol. Symp.* **2006**, 244, 119–125.
- (92) Li, Z.; Chen, C.; Xie, H.; Yao, Y.; Zhang, X.; Brozena, A.; Li, J.; Ding, Y.; Zhao, X.; Hong, M.; et al. Sustainable high-strength macrofibres extracted from natural bamboo. *Nature Sustainability* **2022**, *5*, 235–244.
- (93) Rytioja, J.; Hildén, K.; Yuzon, J.; Hatakka, A.; De Vries, R. P.; Mäkelä, M. R. Plant-Polysaccharide-Degrading Enzymes from Basidiomycetes. *Microbiol. Mol. Biol. Rev.* **2014**, *78*, 614–649.
- (94) Klemm, D.; Kramer, F.; Moritz, S.; Lindström, T.; Ankerfors, M.; Gray, D.; Dorris, A. Nanocelluloses: a New Family of Nature-Based Materials. *Angew. Chem., Int. Ed.* **2011**, *50*, 5438–5466.
- (95) Wu, C.; McClements, D. J.; He, M.; Zheng, L.; Tian, T.; Teng, F.; Li, Y. Preparation and Characterization of Okara Nanocellulose Fabricated Using Sonication or High-Pressure Homogenization Treatments. *Carbohydr. Polym.* **2021**, 255, 117364.
- (96) Klemm, D.; Cranston, E. D.; Fischer, D.; Gama, M.; Kedzior, S. A.; Kralisch, D.; Kramer, F.; Kondo, T.; Lindström, T.; Nietzsche, S.; et al. Nanocellulose as a Natural Source for Groundbreaking Applications in Materials Science: Today's State. *Mater. Today* **2018**, *21*, 720–748.
- (97) Pääkkö, M.; Ankerfors, M.; Kosonen, H.; Nykänen, A.; Ahola, S.; Österberg, M.; Ruokolainen, J.; Laine, J.; Larsson, P. T.; Ikkala, O.; et al. Enzymatic Hydrolysis Combined with Mechanical Shearing and High-Pressure Homogenization for Nanoscale Cellulose Fibrils and Strong Gels. *Biomacromolecules* **2007**, *8*, 1934–1941.
- (98) Henriksson, M.; Henriksson, G.; Berglund, L.; Lindström, T. an Environmentally Friendly Method for Enzyme-Assisted Preparation of Microfibrillated Cellulose (MFC) Nanofibers. *Eur. Polym. J.* **2007**, *43*, 3434–3441.
- (99) Wågberg, L.; Winter, L.; Ödberg, L.; Lindström, T. on the Charge Stoichiometry Upon Adsorption of a Cationic Polyelectrolyte on Cellulosic Materials. *Colloids Surf.* **1987**, *27*, 163–173.
- (100) Isogai, A.; Saito, T.; Fukuzumi, H. TEMPO-Oxidized Cellulose Nanofibers. *Nanoscale* **2011**, *3*, 71–85.
- (101) Saito, T.; Kimura, S.; Nishiyama, Y.; Isogai, A. Cellulose Nanofibers Prepared by TEMPO-Mediated Oxidation of Native Cellulose. *Biomacromolecules* **2007**, *8*, 2485–2491.
- (102) Ghanadpour, M.; Carosio, F.; Larsson, P. T.; Wågberg, L. Phosphorylated Cellulose Nanofibrils: a Renewable Nanomaterial for the Preparation of Intrinsically Flame-Retardant Materials. *Biomacromolecules* **2015**, *16*, 3399–3410.
- (103) Liimatainen, H.; Visanko, M.; Sirviö, J.; Hormi, O.; Niinimäki, J. Sulfonated Cellulose Nanofibrils Obtained from Wood Pulp through Regioselective Oxidative Bisulfite Pre-Treatment. *Cellulose* **2013**, *20*, 741–749.
- (104) Liimatainen, H.; Visanko, M.; Sirviö, J. A.; Hormi, O. E.; Niinimaki, J. Enhancement of the Nanofibrillation of Wood Cellulose Through Sequential Periodate Chlorite Oxidation. *Biomacromolecules* **2012**, *13*, 1592–1597.

- (105) Olszewska, A.; Eronen, P.; Johansson, L.-S.; Malho, J.-M.; Ankerfors, M.; Lindström, T.; Ruokolainen, J.; Laine, J.; Österberg, M. the Behaviour of Cationic Nanofibrillar Cellulose in Aqueous Media. *Cellulose* **2011**, *18*, 1213–1226.
- (106) Araki, J.; Wada, M.; Kuga, S.; Okano, T. Flow Properties of Microcrystalline Cellulose Suspension Prepared by Acid Treatment of Native Cellulose. *Colloids Surf., A* 1998, 142, 75–82.
- (107) Sadeghifar, H.; Filpponen, I.; Clarke, S. P.; Brougham, D. F.; Argyropoulos, D. S. Production of Cellulose Nanocrystals Using Hydrobromic Acid and Click Reactions on Their Surface. *J. Mater. Sci.* **2011**, *46*, 7344–7355.
- (108) Yu, H.-Y.; Zhang, D.-Z.; Lu, F.-F.; Yao, J. New Approach for Single-Step Extraction of Carboxylated Cellulose Nanocrystals for Their Use as Adsorbents and Flocculants. *ACS Sustainable Chem. Eng.* **2016**, *4*, 2632–2643.
- (109) Camarero Espinosa, S.; Kuhnt, T.; Foster, E. J.; Weder, C. Isolation of Thermally Stable Cellulose Nanocrystals by Phosphoric Acid Hydrolysis. *Biomacromolecules* **2013**, *14*, 1223–1230.
- (110) Chen, L.; Zhu, J.; Baez, C.; Kitin, P.; Elder, T. Highly Thermal-Stable and Functional Cellulose Nanocrystals and Nanofibrils Produced Using Fully Recyclable Organic Acids. *Green Chem.* **2016**, *18*, 3835–3843.
- (111) Tripathi, A.; Ago, M.; Khan, S. A.; Rojas, O. J. Heterogeneous Acetylation of Plant Fibers into Micro-and Nanocelluloses for the Synthesis of Highly Stretchable, Tough, and Water-Resistant Co-Continuous Filaments via Wet-Spinning. *ACS Appl. Mater. Interfaces* **2018**, *10*, 44776–44786.
- (112) Jonoobi, M.; Harun, J.; Mathew, A. P.; Hussein, M. Z. B.; Oksman, K. Preparation of Cellulose Nanofibers with Hydrophobic Surface Characteristics. *Cellulose* **2010**, *17*, 299–307.
- (113) Huang, P.; Wu, M.; Kuga, S.; Wang, D.; Wu, D.; Huang, Y. One-Step Dispersion of Cellulose Nanofibers by Mechanochemical Esterification in an Organic Solvent. *ChemSusChem* **2012**, *5*, 2319–2322
- (114) Kang, X.; Sun, P.; Kuga, S.; Wang, C.; Zhao, Y.; Wu, M.; Huang, Y. Thin Cellulose Nanofiber from Corncob Cellulose And Its Performance in Transparent Nanopaper. *ACS Sustainable Chem. Eng.* **2017**, *5*, 2529–2534.
- (115) Beaumont, M.; Otoni, C. G.; Mattos, B. D.; Koso, T. V.; Abidnejad, R.; Zhao, B.; Kondor, A.; King, A. W.; Rojas, O. J. Regioselective and Water-Assisted Surface Esterification of Never-Dried Cellulose: Nanofibers with Adjustable Surface Energy. *Green Chem.* **2021**, 23, 6966–6974.
- (116) Beaumont, M.; Winklehner, S.; Veigel, S.; Mundigler, N.; Gindl-Altmutter, W.; Potthast, A.; Rosenau, T. Wet Esterification of Never-Dried Cellulose: a Simple Process to Surface-Acetylated Cellulose Nanofibers. *Green Chem.* **2020**, 22, 5605–5609.
- (117) Beaumont, M.; Tardy, B. L.; Reyes, G.; Koso, T. V.; Schaubmayr, E.; Jusner, P.; King, A. W.; Dagastine, R. R.; Potthast, A.; Rojas, O. J. Assembling Native Elementary Cellulose Nanofibrils via a Reversible and Regioselective Surface Functionalization. *J. Am. Chem. Soc.* 2021, 143, 17040.
- (118) Beaumont, M.; Jusner, P.; Gierlinger, N.; King, A. W.; Potthast, A.; Rojas, O. J.; Rosenau, T. Unique Reactivity of Nanoporous Cellulosic Materials Mediated by Surface-Confined Water. *Nat. Commun.* **2021**, *12*, 1–8.
- (119) Brinkmann, A.; Chen, M.; Couillard, M.; Jakubek, Z. J.; Leng, T.; Johnston, L. J. Correlating Cellulose Nanocrystal Particle Size and Surface Area. *Langmuir* **2016**, *32*, 6105–6114.
- (120) Ogawa, Y.; Putaux, J.-L. Transmission Electron Microscopy of Cellulose. Part 2: Technical and Practical Aspects. *Cellulose* **2019**, *26*, 17–34.
- (121) Salem, K. S.; Starkey, H. R.; Pal, L.; Lucia, L.; Jameel, H. the Topochemistry of Cellulose Nanofibrils as a Function of Mechanical Generation Energy. *ACS Sustainable Chem. Eng.* **2020**, *8*, 1471–1478. (122) Tanaka, R.; Saito, T.; Ishii, D.; Isogai, A. Determination of Nanocellulose Fibril Length by Shear Viscosity Measurement. *Cellulose* **2014**, *21*, 1581–1589.

- (123) Zhou, Y.; Fujisawa, S.; Saito, T.; Isogai, A. Characterization of Concentration-Dependent Gelation Behavior of Aqueous 2, 2, 6, 6-Tetramethylpiperidine-1-Oxyl— Cellulose Nanocrystal Dispersions Using Dynamic Light Scattering. *Biomacromolecules* 2019, 20, 750—757
- (124) Chinga-Carrasco, G. Potential and Limitations of Nanocelluloses as Components in Biocomposite Inks for Three-Dimensional Bioprinting and for Biomedical Devices. *Biomacromolecules* **2018**, *19*, 701–711.
- (125) Qian, J.; Chen, Q.; Hong, M.; Xie, W.; Jing, S.; Bao, Y.; Chen, G.; Pang, Z.; Hu, L.; Li, T. Toward Stretchable Batteries: 3D-Printed Deformable Electrodes and Separator Enabled by Nanocellulose. *Mater. Today* **2022**, *54*, 18.
- (126) Zhu, P.; Yu, Z.; Sun, H.; Zheng, D.; Zheng, Y.; Qian, Y.; Wei, Y.; Lee, J.; Srebnik, S.; Chen, W. 3D Printed Cellulose Nanofiber Aerogel Scaffold With Hierarchical Porous Structures for Fast Solar-Driven Atmospheric Water Harvesting. *Adv. Mater.* **2023**, e2306653–e2306653A.
- (127) Cao, D.; Xing, Y.; Tantratian, K.; Wang, X.; Ma, Y.; Mukhopadhyay, A.; Cheng, Z.; Zhang, Q.; Jiao, Y.; Chen, L.; et al. 3D Printed High-Performance Lithium Metal Microbatteries Enabled by Nanocellulose. *Adv. Mater.* **2019**, *31*, 1807313.
- (128) Chen, L.; He, S.; Huang, W.; Liu, D.; Bi, T.; Zhang, C.; Chen, C. 3D-Printed Tripodal Porous Wood-Mimetic Cellulosic Composite Evaporator for Salt-Free Water Desalination. *Composites, Part B* **2023**, 263, 110830.
- (129) Yu, L.; Gao, T.; Mi, R.; Huang, J.; Kong, W.; Liu, D.; Liang, Z.; Ye, D.; Chen, C. 3D-Printed Mechanically Strong and Extreme Environment Adaptable Boron Nitride/Cellulose Nanofluidic Macrofibers. *Nano Res.* **2023**, *16*, 7609.
- (130) Sydney Gladman, A.; Matsumoto, E. A.; Nuzzo, R. G.; Mahadevan, L.; Lewis, J. A. Biomimetic 4D Printing. *Nat. Mater.* **2016**, *15*, 413–418.
- (131) Dai, L.; Cheng, T.; Duan, C.; Zhao, W.; Zhang, W.; Zou, X.; Aspler, J.; Ni, Y. 3D Printing Using Plant-Derived Cellulose and Its Derivatives: A Review. *Carbohydr. Polym.* **2019**, 203, 71–86.
- (132) Tanaka, R.; Saito, T.; Hondo, H.; Isogai, A. Influence of Flexibility and Dimensions of Nanocelluloses on the Flow Properties of Their Aqueous Dispersions. *Biomacromolecules* **2015**, *16*, 2127–2131.
- (133) Siqueira, G.; Kokkinis, D.; Libanori, R.; Hausmann, M. K.; Gladman, A. S.; Neels, A.; Tingaut, P.; Zimmermann, T.; Lewis, J. A.; Studart, A. R. Cellulose Nanocrystal Inks for 3D Printing of Textured Cellular Architectures. *Adv. Eng. Mater.* **2017**, *27*, 1604619.
- (134) Hausmann, M. K.; Siqueira, G.; Libanori, R.; Kokkinis, D.; Neels, A.; Zimmermann, T.; Studart, A. R. Complex-Shaped Cellulose Composites Made by Wet Densification of 3D Printed Scaffolds. *Adv. Funct. Mater.* **2020**, *30*, 1904127.
- (135) Hu, L.; Zhong, Y.; Wu, S.; Wei, P.; Huang, J.; Xu, D.; Zhang, L.; Ye, Q.; Cai, J. Biocompatible and Biodegradable Super-Toughness Regenerated Cellulose via Water Molecule-Assisted Molding. *Chem. Eng. J.* **2021**, 417, 129229.
- (136) Han, X.; Wang, Z.; Ding, L.; Chen, L.; Wang, F.; Pu, J.; Jiang, S. Water Molecule-Induced Hydrogen Bonding between Cellulose Nanofibers Toward Highly Strong and Tough Materials from Wood Aerogel. *Chin. Chem. Lett.* **2021**, 32, 3105–3108.
- (137) Han, X.; Wu, W.; Wang, J.; Tian, Z.; Jiang, S. Hydrogen-Bonding-Aided Fabrication of Wood Derived Cellulose Scaffold/Aramid Nanofiber into High-Performance Bulk Material. *Materials* **2021**, *14*, 5444.
- (138) Han, X.; Ye, Y.; Lam, F.; Pu, J.; Jiang, F. Hydrogen-Bonding-Induced Assembly of Aligned Cellulose Nanofibers into Ultrastrong and Tough Bulk Materials. *J. Mater. Chem. A* **2019**, *7*, 27023–27031.
- (139) Jiang, F.; Liu, H.; Li, Y.; Kuang, Y.; Xu, X.; Chen, C.; Huang, H.; Jia, C.; Zhao, X.; Hitz, E.; Zhou, Y.; Yang, R.; Cui, L.; Hu, L. Lightweight, Mesoporous, and Highly Absorptive All-Nanofiber Aerogel for Efficient Solar Steam Generation. ACS Appl. Mater. Interfaces 2018, 10, 1104–1112.

- (140) Chen, Y.; Yu, Z.; Ye, Y.; Zhang, Y.; Li, G.; Jiang, F. Superelastic, Hygroscopic, and Ionic Conducting Cellulose Nanofibril Monoliths by 3D Printing. *ACS Nano* **2021**, *15*, 1869–1879.
- (141) Sinquefield, S.; Ciesielski, P. N.; Li, K.; Gardner, D. J.; Ozcan, S. Nanocellulose Dewatering and Drying: Current State and Future Perspectives. *ACS Sustainable Chem. Eng.* **2020**, *8*, 9601–9615.
- (142) Rol, F.; Billot, M.; Bolloli, M.; Beneventi, D.; Bras, J. Production of 100% Cellulose Nanofibril Objects Using the Molded Cellulose Process: a Feasibility Study. *Ind. Eng. Chem. Res.* **2020**, 59, 7670–7679.
- (143) Xiao, J.; Li, H.; Zhang, H.; He, S.; Zhang, Q.; Liu, K.; Jiang, S.; Duan, G.; Zhang, K. Nanocellulose and Its Derived Composite Electrodes toward Supercapacitors: Fabrication, Properties, and Challenges. J. Bioresour. Bioprod. 2022, 7, 245–269.
- (144) Dimic-Misic, K.; Puisto, A.; Paltakari, J.; Alava, M.; Maloney, T. the Influence of Shear on the Dewatering of High Consistency Nanofibrillated Cellulose Furnishes. *Cellulose* **2013**, *20*, 1853–1864.
- (145) Dimic-Misic, K.; Puisto, A.; Gane, P.; Nieminen, K.; Alava, M.; Paltakari, J.; Maloney, T. the Role of MFC/NFC Swelling in the Rheological Behavior and Dewatering of High Consistency Furnishes. *Cellulose* **2013**, *20*, 2847–2861.
- (146) Dimic-Misic, K.; Maloney, T.; Liu, G.; Gane, P. Micro Nanofibrillated Cellulose (MNFC) Gel Dewatering Induced at Ultralow-Shear in Presence of Added Colloidally-Unstable Particles. *Cellulose* **2017**, *24*, 1463–1481.
- (147) Dimic-Misic, K.; Maloney, T.; Gane, P. Effect of Fibril Length, Aspect Ratio and Surface Charge on Ultralow Shear-Induced Structuring in Micro and Nanofibrillated Cellulose Aqueous Suspensions. *Cellulose* **2018**, 25, 117–136.
- (148) Li, Z.; Chen, C.; Xie, H.; Yao, Y.; Zhang, X.; Brozena, A.; Li, J.; Ding, Y.; Zhao, X.; Hong, M. Sustainable High-Strength Macrofibres Extracted from Natural Bamboo. *Nature Sustainability* **2022**, *5*, 235.
- (149) Etale, A.; Onyianta, A. J.; Turner, S. R.; Eichhorn, S. J. Cellulose: a Review of Water Interactions, Applications in Composites, and Water Treatment. *Chem. Rev.* **2023**, *123*, 2016.
- (150) Peng, Y.; Han, Y.; Gardner, D. J. Spray-Drying Cellulose Nanofibrils: Effect of Drying Process Parameters on Particle Morphology and Size Distribution. *Wood Fiber Sci.* **2012**, *44*, 448–461.
- (151) Chen, C.; Li, Z.; Mi, R.; Dai, J.; Xie, H.; Pei, Y.; Li, J.; Qiao, H.; Tang, H.; Yang, B.; et al. Rapid Processing of Whole Bamboo with Exposed, Aligned Nanofibrils toward a High-Performance Structural Material. ACS Nano 2020, 14, 5194–5202.
- (152) Vongpradubchai, S.; Rattanadecho, P. the Microwave Processing of Wood Using a Continuous Microwave Belt Drier. *Chem. Eng. Process.: Process Intensif.* **2009**, 48, 997–1003.
- (153) Oloyede, A.; Groombridge, P. the Influence of Microwave Heating on the Mechanical Properties of Wood. *J. Mater. Process. Technol.* **2000**, *100*, *67*–73.
- (154) Peng, Y.; Gardner, D. J.; Han, Y. Drying Cellulose Nanofibrils: in Search of a Suitable Method. *Cellulose* **2012**, *19*, 91–102.
- (155) Pelton, R. a Model of the External Surface of Wood Pulp Fibers. Nord. Pulp Pap. Res. J. 1993, 8, 113-119.
- (156) Jiménez-Saelices, C.; Seantier, B.; Cathala, B.; Grohens, Y. Spray Freeze-Dried Nanofibrillated Cellulose Aerogels with Thermal Superinsulating Properties. *Carbohydr. Polym.* **2017**, *157*, 105–113.
- (157) Yang, J.; Han, X.; Yang, W.; Hu, J.; Zhang, C.; Liu, K.; Jiang, S. Nanocellulose-Based Composite Aerogels toward the Environmental Protection: Preparation, Modification and Applications. *Environ. Res.* **2023**, 236, 116736.
- (158) Si, R.; Pu, J.; Luo, H.; Wu, C.; Duan, G. Nanocellulose-Based Adsorbents for Heavy Metal Ion. *Polymers* **2022**, *14*, 5479.
- (159) Mi, H.-Y.; Jing, X.; Politowicz, A. L.; Chen, E.; Huang, H.-X.; Turng, L.-S. Highly Compressible Ultra-Light Anisotropic Cellulose/Graphene Aerogel Fabricated by Bidirectional Freeze Drying for Selective Oil Absorption. *Carbon* **2018**, *132*, 199–209.
- (160) Zhuo, H.; Hu, Y.; Tong, X.; Chen, Z.; Zhong, L.; Lai, H.; Liu, L.; Jing, S.; Liu, Q.; Liu, C.; et al. a Supercompressible, Elastic, and

- Bendable Carbon Aerogel with Ultrasensitive Detection Limits for Compression Strain, Pressure, and Bending Angle. *Adv. Mater.* **2018**, 30, 1706705.
- (161) Zhang, X.; Zhao, X.; Xue, T.; Yang, F.; Fan, W.; Liu, T. Bidirectional Anisotropic Polyimide/Bacterial Cellulose Aerogels by Freeze-Drying for Super-Thermal Insulation. *Chem. Eng. J.* **2020**, 385, 123963.
- (162) Chen, Y.; Li, S.; Li, X.; Mei, C.; Zheng, J.; E, S.; Duan, G.; Liu, K.; Jiang, S. Liquid Transport and Real-Time Dye Purification via Lotus Petiole-Inspired Long-Range-Ordered Anisotropic Cellulose Nanofibril Aerogels. *ACS Nano* **2021**, *15*, 20666–20677.
- (163) Chen, Y.; Hanshe, M.; Sun, Z.; Zhou, Y.; Mei, C.; Duan, G.; Zheng, J.; Shiju, E.; Jiang, S. Lightweight and Anisotropic Cellulose Nanofibril/Rectorite Composite Sponges for Efficient Dye Adsorption and Selective Separation. *Int. J. Biol. Macromol.* **2022**, 207, 130–139
- (164) Chen, Y.; Luo, H.; Guo, H.; Liu, K.; Mei, C.; Li, Y.; Duan, G.; He, S.; Han, J.; Zheng, J.; et al. Anisotropic Cellulose Nanofibril Composite Sponges for Electromagnetic Interference Shielding with Low Reflection Loss. *Carbohydr. Polym.* **2022**, *276*, 118799.
- (165) Huang, Y.; Kasuga, T.; Nogi, M.; Koga, H. Clearly Transparent and Air-Permeable Nanopaper with Porous Structures Consisting of TEMPO-Oxidized Cellulose Nanofibers. *RSC Adv.* **2023**, *13*, 21494–21501.
- (166) Han, X.; Wang, J.; Wang, J.; Ding, L.; Zhang, K.; Han, J.; Jiang, S. Micro- and Nano-Fibrils of Manau Rattan and Solvent-Exchange-Induced High-Haze Transparent Holocellulose Nanofibril Film. *Carbohydr. Polym.* **2022**, 298, 120075.
- (167) Zeng, Z.; Wang, C.; Wu, T.; Han, D.; Luković, M.; Pan, F.; Siqueira, G.; Nyström, G. Nanocellulose Assisted Preparation of Ambient Dried, Large-Scale and Mechanically Robust Carbon Nanotube Foams for Electromagnetic Interference Shielding. *J. Mater. Chem. A* **2020**, *8*, 17969–17979.
- (168) Sun, L.; Liu, L.; Wu, M.; Wang, D.; Shen, R.; Zhao, H.; Lu, J.; Yao, J. Nanocellulose Interface Enhanced All-Cellulose Foam with Controllable Strength via a Facile Liquid Phase Exchange Route. *Carbohydr. Polym.* **2023**, 299, 120192.
- (169) Sethi, J.; Oksman, K.; Illikainen, M.; Sirviö, J. A. Sonication-Assisted Surface Modification Method to Expedite the Water Removal from Cellulose Nanofibers for Use in Nanopapers and Paper Making. *Carbohydr. Polym.* **2018**, *197*, 92–99.
- (170) Sim, K.; Lee, J.; Lee, H.; Youn, H. J. Flocculation Behavior of Cellulose Nanofibrils Under Different Salt Conditions and Its Impact On Network Strength and Dewatering Ability. *Cellulose* **2015**, *22*, 3689–3700.
- (171) Françon, H.; Wang, Z.; Marais, A.; Mystek, K.; Piper, A.; Granberg, H.; Malti, A.; Gatenholm, P.; Larsson, P. A.; Wågberg, L. Ambient-Dried, 3D-Printable and Electrically Conducting Cellulose Nanofiber Aerogels by Inclusion of Functional Polymers. *Adv. Funct. Mater.* **2020**, *30*, 1909383.
- (172) Sakuma, W.; Yamasaki, S.; Fujisawa, S.; Kodama, T.; Shiomi, J.; Kanamori, K.; Saito, T. Mechanically Strong, Scalable, Mesoporous Xerogels of Nanocellulose Featuring Light Permeability, Thermal Insulation, and Flame Self-Extinction. ACS Nano 2021, 15, 1436—1444.
- (173) Wang, R.; Chen, C.; Pang, Z.; Wang, X.; Zhou, Y.; Dong, Q.; Guo, M.; Gao, J.; Ray, U.; Xia, Q. Fabrication of Cellulose-Graphite Foam via Ion Cross-Linking and Ambient-Drying. *Nano Lett.* **2022**, 22, 3931.
- (174) Chen, C.; Zhou, Y.; Xie, W.; Meng, T.; Zhao, X.; Pang, Z.; Chen, Q.; Liu, D.; Wang, R.; Yang, V.; et al. Lightweight, Thermally Insulating, Fire-Proof Graphite-Cellulose Foam. *Adv. Funct. Mater.* **2023**, 33, 2204219.
- (175) Wang, S.; Yu, L.; Wang, S.; Zhang, L.; Chen, L.; Xu, X.; Song, Z.; Liu, H.; Chen, C. Strong, Tough, Ionic Conductive, and Freezing-Tolerant All-Natural Hydrogel Enabled by Cellulose-Bentonite Coordination Interactions. *Nat. Commun.* **2022**, *13*, 1–11.
- (176) Chen, L.; Wang, S.; Wang, S.; Chen, C.; Qi, L.; Yu, L.; Lu, Z.; Huang, J.; Chen, J.; Wang, Z.; et al. Scalable Production of

- Biodegradable, Recyclable, Sustainable Cellulose-Mineral Foams via Coordination Interaction Assisted Ambient Drying. ACS Nano 2022, 16, 16414–16425.
- (177) Xu, Y.; Xu, Y.; Chen, H.; Gao, M.; Yue, X.; Ni, Y. Redispersion of Dried Plant Nanocellulose: a Review. *Carbohydr. Polym.* **2022**, 294, 119830.
- (178) Chen, Y.; Zhou, L.; Chen, L.; Duan, G.; Mei, C.; Huang, C.; Han, J.; Jiang, S. Anisotropic Nanocellulose Aerogels with Ordered Structures Fabricated by Directional Freeze-Drying for Fast Liquid Transport. *Cellulose* **2019**, *26*, 6653–6667.
- (179) Li, Y.; Zhu, H.; Wang, Y.; Ray, U.; Zhu, S.; Dai, J.; Chen, C.; Fu, K.; Jang, S. H.; Henderson, D.; et al. Cellulose-Nanofiber-Enabled 3D Printing of a Carbon-Nanotube Microfiber Network. *Small Methods* **2017**, *1*, 1700222.
- (180) Wang, L.; Lundahl, M. J.; Greca, L. G.; Papageorgiou, A. C.; Borghei, M.; Rojas, O. J. Effects of Non-Solvents and Electrolytes on the Formation and Properties of Cellulose I Filaments. *Sci. Rep.* **2019**, *9*, 1–11.
- (181) Osong, S. H.; Norgren, S.; Engstrand, P. Processing of Wood-Based Microfibrillated Cellulose and Nanofibrillated Cellulose, and Applications Relating to Papermaking: a Review. *Cellulose* **2016**, 23, 93–123.
- (182) Kalia, S.; Boufi, S.; Celli, A.; Kango, S. Nanofibrillated Cellulose: Surface Modification and Potential Applications. *Colloid Polym. Sci.* **2014**, 292, 5–31.
- (183) Mittal, N.; Ansari, F.; Gowda, V. K.; Brouzet, C.; Chen, P.; Larsson, P. T.; Roth, S. V.; Lundell, F.; Wagberg, L.; Kotov, N. A; Söderberg, L. D.; et al. Multiscale Control of Nanocellulose Assembly: Transferring Remarkable Nanoscale Fibril Mechanics to Macroscale Fibers. ACS Nano 2018, 12, 6378–6388.
- (184) Håkansson, K. M.; Fall, A. B.; Lundell, F.; Yu, S.; Krywka, C.; Roth, S. V.; Santoro, G.; Kvick, M.; Prahl Wittberg, L.; Wågberg, L.; Söderberg, L. D. Hydrodynamic Alignment and Assembly of Nanofibrils Resulting in Strong Cellulose Filaments. *Nat. Commun.* **2014**. *5*, 4018.
- (185) Sakurada, I.; Nukushina, Y.; Ito, T. Experimental Determination of the Elastic Modulus of Crystalline Regions in Oriented Polymers. *J. Polym. Sci.* **1962**, *57*, 651–660.
- (186) Tashiro, K.; Kobayashi, M. Theoretical Evaluation of Three-Dimensional Elastic Constants of Native and Regenerated Celluloses: Role of Hydrogen Bonds. *Polymer* 1991, 32, 1516–1526.
- (187) Wainwright, S. A.; Biggs, W.; Currey, J. D. Mechanical Design in Organisms; Princeton University Press: 1982.
- (188) Zimmermann, T.; Pöhler, E.; Geiger, T. Cellulose Fibrils for Polymer Reinforcement. Adv. Eng. Mater. 2004, 6, 754–761.
- (189) Zhu, H.; Zhu, S.; Jia, Z.; Parvinian, S.; Li, Y.; Vaaland, O.; Hu, L.; Li, T. Anomalous Scaling Law of Strength and Toughness of Cellulose Nanopaper. *Proc. Natl. Acad. Sci.* **2015**, *112*, 8971–8976.
- (190) Kuang, Y.; Chen, C.; Cheng, J.; Pastel, G.; Li, T.; Song, J.; Jiang, F.; Li, Y.; Zhang, Y.; Jang, S.-H.; et al. Selectively Aligned Cellulose Nanofibers towards High-Performance Soft Actuators. *Extreme Mechanics Letters* **2019**, 29, 100463.
- (191) Lundahl, M. J.; Cunha, A. G.; Rojo, E.; Papageorgiou, A. C.; Rautkari, L.; Arboleda, J. C.; Rojas, O. J. Strength and Water Interactions of Cellulose I Filaments Wet-Spun from Cellulose Nanofibril Hydrogels. *Sci. Rep.* **2016**, *6*, 1–13.
- (192) Benítez, A. J.; Torres-Rendon, J.; Poutanen, M.; Walther, A. Humidity and Multiscale Structure Govern Mechanical Properties and Deformation Modes in Films of Native Cellulose Nanofibrils. *Biomacromolecules* **2013**, *14*, 4497–4506.
- (193) Petridis, L.; O'Neill, H. M.; Johnsen, M.; Fan, B.; Schulz, R.; Mamontov, E.; Maranas, J.; Langan, P.; Smith, J. C. Hydration Control of the Mechanical and Dynamical Properties of Cellulose. *Biomacromolecules* **2014**. *15*, 4152–4159.
- (194) Nakamura, K.; Hatakeyama, T.; Hatakeyama, H. Effect of Bound Water on Tensile Properties of Native Cellulose. *Text. Res. J.* 1983, 53, 682–688.

- (195) Baley, C.; Morvan, C.; Grohens, Y. Influence of the Absorbed Water on the Tensile Strength of Flax Fibers. *Macromol. Symp.* **2005**, 222, 195–202.
- (196) Hou, Y.; Guan, Q.-F.; Xia, J.; Ling, Z.-C.; He, Z.; Han, Z.-M.; Yang, H.-B.; Gu, P.; Zhu, Y.; Yu, S.-H. Strengthening and Toughening Hierarchical Nanocellulose via Humidity-Mediated Interface. ACS Nano 2021, 15, 1310.
- (197) Sahputra, I. H.; Alexiadis, A.; Adams, M. J. Effects of Moisture on the Mechanical Properties of Microcrystalline Cellulose and the Mobility of the Water Molecules as Studied by the Hybrid Molecular Mechanics—Molecular Dynamics Simulation Method. *J. Polym. Sci., Part B: Polym. Phys.* **2019**, *57*, 454–464.
- (198) Chen, C.; Hu, L. Nanoscale Ion Regulation in Wood-Based Structures and Their Device Applications. *Adv. Mater.* **2021**, 33, 2002890.
- (199) Chen, G.; Li, T.; Chen, C.; Wang, C.; Liu, Y.; Kong, W.; Liu, D.; Jiang, B.; He, S.; Kuang, Y.; et al. a Highly Conductive Cationic Wood Membrane. *Adv. Funct. Mater.* **2019**, *29*, 1902772.
- (200) Li, T.; Li, S. X.; Kong, W.; Chen, C.; Hitz, E.; Jia, C.; Dai, J.; Zhang, X.; Briber, R.; Siwy, Z.; et al. a Nanofluidic Ion Regulation Membrane with Aligned Cellulose Nanofibers. *Sci. Adv.* **2019**, *5*, No. eaau4238.
- (201) Zhou, Y.; Chen, C.; Zhang, X.; Liu, D.; Xu, L.; Dai, J.; Liou, S.-C.; Wang, Y.; Li, C.; Xie, H.; et al. Decoupling Ionic and Electronic Pathways in Low-Dimensional Hybrid Conductors. *J. Am. Chem. Soc.* **2019**, *141*, 17830–17837.
- (202) Ye, Y.; Yu, L.; Lizundia, E.; Zhu, Y.; Chen, C.; Jiang, F. Cellulose-Based Ionic Conductor: an Emerging Material toward Sustainable Devices. *Chem. Rev.* **2023**, *123*, 9204–9264.
- (203) Huang, J.; Yu, L.; Wang, S.; Qi, L.; Lu, Z.; Chen, L.; Xu, D.; Deng, H.; Chen, C. an Ultrathin Nanocellulosic Ion Redistributor for Long-Life Zinc Anode. *Innov. Mater.* **2023**, *1*, 100029.
- (204) Tao, J.; Jiao, L.; Deng, Y. Cellulose-and Nanocellulose-Based Dielectric Materials. In *Nanocellulose Based Composites for Electronics*; Elsevier, 2021; pp 73–100.
- (205) Inui, T.; Koga, H.; Nogi, M.; Komoda, N.; Suganuma, K. a Miniaturized Flexible Antenna Printed on a High Dielectric Constant Nanopaper Composite. *Adv. Mater.* **2015**, *27*, 1112–1116.
- (206) Inui, T.; Koga, H.; Nogi, M.; Komoda, N.; Suganuma, K. High-Dielectric Paper Composite Consisting of Cellulose Nanofiber and Silver Nanowire. In *14th IEEE international conference on nanotechnology*; IEEE: 2014; pp 470–473.
- (207) Tobjörk, D.; Österbacka, R. Paper Electronics. *Adv. Mater.* **2011**, 23, 1935–1961.
- (208) Huang, J.; Zhou, Y.; Dong, L.; Zhou, Z.; Liu, R. Enhancement of Mechanical and Electrical Performances of Insulating Presspaper by Introduction of Nanocellulose. *Compos. Sci. Technol.* **2017**, *138*, 40–48.
- (209) Klemenčič, D.; Simončič, B.; Tomšič, B.; Orel, B. Biodegradation of Silver Functionalised Cellulose Fibres. *Carbohydr. Polym.* **2010**, *80*, 426–435.
- (210) Tanaka, M.; Hayashi, T.; Morita, S. the Roles of Water Molecules at the Biointerface of Medical Polymers. *Polym. J.* **2013**, *45*, 701–710.
- (211) Tomšič, B.; Simončič, B.; Orel, B.; Vilčnik, A.; Spreizer, H. Biodegradability of Cellulose Fabric Modified by Imidazolidinone. *Carbohydr. Polym.* **2007**, *69*, 478–488.
- (212) Montegut, D.; Indictor, N.; Koestler, R. J. Fungal Deterioration of Cellulosic Textiles: a Review. *Int. Biodeterior.* **1991**, 28, 209–226.
- (213) Park, C. H.; Kang, Y. K.; Im, S. S. Biodegradability of Cellulose Fabrics. J. Appl. Polym. Sci. 2004, 94, 248–253.
- (214) Vilcnik, A.; Jerman, I.; Surca Vuk, A.; Kozelj, M.; Orel, B.; Tomsic, B.; Simoncic, B.; Kovac, J. Structural Properties and Antibacterial Effects of Hydrophobic and Oleophobic Sol-Gel Coatings for Cotton Fabrics. *Langmuir* **2009**, 25, 5869–5880.
- (215) Rimdusit, S.; Jingjid, S.; Damrongsakkul, S.; Tiptipakorn, S.; Takeichi, T. Biodegradability and Property Characterizations of

- Methyl Cellulose: Effect of Nanocompositing and Chemical Crosslinking. *Carbohydr. Polym.* **2008**, 72, 444–455.
- (216) Takeuchi, Y.; Khawdas, W.; Aso, Y.; Ohara, H. Microbial Fuel Cells Using Cellulomonas Spp. with Cellulose as Fuel. *J. Biosci. Bioeng.* **2017**, *123*, 358–363.
- (217) Pant, D.; Van Bogaert, G.; Diels, L.; Vanbroekhoven, K. a Review of the Substrates Used In Microbial Fuel Cells (MFCs) For Sustainable Energy Production. *Bioresour. Technol.* **2010**, *101*, 1533–1543.
- (218) Cheng, S.; Kiely, P.; Logan, B. E. Pre-Acclimation of a Wastewater Inoculum to Cellulose in an Aqueous-Cathode MEC Improves Power Generation in Air-Cathode MFCs. *Bioresour. Technol.* **2011**, *102*, 367–371.
- (219) Ahmad, F.; Atiyeh, M. N.; Pereira, B.; Stephanopoulos, G. N. a Review of Cellulosic Microbial Fuel Cells: Performance and Challenges. *Biomass Bioenergy* **2013**, *56*, 179–188.
- (220) Wang, J.; Han, X.; Zhang, C.; Liu, K.; Duan, G. Source of Nanocellulose and Its Application in Nanocomposite Packaging Material: a Review. *Nanomaterials* **2022**, *12*, 3158.
- (221) Malešič, J.; Kolar, J.; Strlič, M.; Kočar, D.; Fromageot, D.; Lemaire, J.; Haillant, O. Photo-Induced Degradation of Cellulose. *Polym. Degrad. Stab.* **2005**, *89*, 64–69.
- (222) Hon, D. N. S. Photooxidative Degradation of Cellulose: Reactions of the Cellulosic Free Radicals with Oxygen. *J. Polym. Sci., Polym. Chem. Ed.* **1979**, *17*, 441–454.
- (223) Schuchmann, M. N.; von Sonntag, C. Radiation Chemistry of Carbohydrates. Part 14. Hydroxyl Radical Induced Oxidation of D-Glucose in Oxygenated Aqueous Solution. *J. Chem. Soc., Perkin Trans.* 1977, 2, 1958–1963.
- (224) Solhi, L.; Guccini, V.; Heise, K.; Solala, I.; Niinivaara, E.; Xu, W.; Mihhels, K.; Kröger, M.; Meng, Z.; Wohlert, J.; et al. Understanding Nanocellulose-Water Interactions: Turning a Detriment into an Asset. *Chem. Rev.* **2023**, *123*, 1925–2015.
- (225) Xia, Q.; Chen, C.; Yao, Y.; Li, J.; He, S.; Zhou, Y.; Li, T.; Pan, X.; Yao, Y.; Hu, L. a Strong, Biodegradable and Recyclable Lignocellulosic Bioplastic. *Nature Sustainability* **2021**, *4*, 627–635.
- (226) Zhao, D.; Zhu, Y.; Cheng, W.; Xu, G.; Wang, Q.; Liu, S.; Li, J.; Chen, C.; Yu, H.; Hu, L. a Dynamic Gel with Reversible and Tunable Topological Networks and Performances. *Matter* **2020**, *2*, 390–403.
- (227) Zhao, D.; Pang, B.; Zhu, Y.; Cheng, W.; Cao, K.; Ye, D.; Si, C.; Xu, G.; Chen, C.; Yu, H. a Stiffness-Switchable, Biomimetic Smart Material Enabled by Supramolecular Reconfiguration. *Adv. Mater.* **2022**, *34*, 2107857.
- (228) Han, N.; Zhang, J.; Hoang, M.; Gray, S.; Xie, Z. a Review of Process and Wastewater Reuse in the Recycled Paper Industry. *Environ. Technol. Innovation* **2021**, 24, 101860.